

Thermorefringent noise in crystalline optical materials

Serhii Kryhin¹,¹ Evan D. Hall,^{1,2} and Vivishek Sudhir^{2,3}

¹*Department of Physics, Massachusetts Institute of Technology, Cambridge, Massachusetts 02139, USA*

²*LIGO Laboratory, Massachusetts Institute of Technology, Cambridge, Massachusetts 02139, USA*

³*Department of Mechanical Engineering, Massachusetts Institute of Technology, Cambridge, Massachusetts 02139, USA*



(Received 18 November 2021; accepted 21 November 2022; published 3 January 2023)

Crystalline materials are increasingly employed to construct precision optical instruments because of their reduced mechanical dissipation and consequent reduction of thermal Brownian noise. However, the anisotropy of the crystalline state implies a fundamental source of thermal noise; depolarization induced by thermal fluctuations of its birefringence. We establish the theory of this effect, which is a generalization of prior treatments of thermo-optic noises in amorphous materials. This theory—in conjunction with poorly understood anisotropic thermal stress coefficients of crystalline coatings—predict that thermo-refringent noise in crystalline mirror coatings may be lurking within an order of magnitude of Brownian noise (below 100 Hz). Thus, in order to appreciate the full promise of crystalline optical materials, a more precise understanding of their anisotropic material constants is necessary. Barring that, we elucidate measurement techniques that can affect partial coherent cancellation of thermorefringent noise. In passing, our general formalism also predicts the existence of thermal beam-pointing noise.

DOI: [10.1103/PhysRevD.107.022001](https://doi.org/10.1103/PhysRevD.107.022001)

I. INTRODUCTION

Optical media are surprisingly active even at arbitrarily low light intensity. Dissipation—thermal, mechanical, and optical—leads to fluctuations in the optical fields that interact with them [1]. For example, thermal dissipation in optical media produces apparent temperature fluctuations that cause fluctuations in their refractive index and length [2–4]. The combination of such thermorefractive and thermoelastic noises—so-called thermo-optic noise [5]—limits the sensitivity of optical fiber strain sensors [6,7], the frequency stability of fiber lasers [8,9], and the utility of micro and nanophotonic components [10–15]. On the other hand, mechanical dissipation in optical media produces fluctuations in the material strain. Such Brownian noise in cavity spacers, mirror substrates, and reflective coatings [16] limits the stability of optical atomic clocks [17–20] and the sensitivity of interferometric gravitational-wave detectors [21–25]. (Noise due to optical dissipation, via the photothermoelastic and photothermorefractive mechanisms [26], have so far only been circumstantially implicated [27].) The common feature of these observations is the role of the amorphous character of optical materials.

In this context, crystalline optical materials have gained a reputation for their reduced Brownian noise [28,29]. The nature of thermo-optic noise in crystalline materials must be understood before the full extent of their promise can be imagined. However, prior theories of thermo-optic noise [4,5,16,26,30–34] focus on thermodynamic fluctuations in

isotropic materials which do not directly apply to crystalline materials (while prior measurements on a crystalline micro-cavity [35] were apparently limited by thermorefractive noise). Indeed, the hallmark of the crystalline state is the anisotropy of its physical properties. In particular, both its thermal and optical responses can be anisotropic, implying that thermodynamic fluctuations of its optical properties can be qualitatively different from those of amorphous materials.

We show that anisotropic optical materials—exemplified by crystalline media—exhibit a more complicated fluctuation of their apparent temperature than do isotropic materials. In turn, this induces new types of noise in the electromagnetic field, such as the appearance of noise in polarization modes orthogonal to the polarization of the incident mode. In general, the polarization state of light acquires a noisy character, an effect we dub *thermorefringent noise*. Interference of such a noisy state of light with any independent reference will be imperfect, so that thermorefringent noise can appear as apparent amplitude and phase noise, which makes it particularly treacherous and qualitatively different from thermo-optic noise in amorphous material (which appear as apparent phase noise only). Indeed, the improved Brownian thermal noise performance of crystalline coatings [28] may ultimately be limited by thermorefringent noise. Recent measurements have in fact discovered excess noise in optical cavities made of crystalline coatings that is thought to be due to polarization fluctuations [36].

Our predictions apply equally to optical materials which can develop small anisotropies due to induced strain. This perspective is particularly germane to precision optical polarimetry [37–41], such as for tests of QED [42,43], and optical searches for physics beyond the Standard Model [44–46].

In addition to thermorefringent noise, the first-principles formalism we develop allows us to uncover the possibility of thermodynamically-induced scattering into higher-order spatial modes, an effect that must also exist in amorphous media, but has not been considered so far.

We finally introduce balanced homodyne polarimetry, a polarization sensitive variant of homodyne detection that can affect coherent cancellation of thermorefringent noise. This technique of reducing the impact of optical thermal noise is agnostic to precise details of the coating layers or materials (in contrast to coating layer or material engineering techniques [32–34,47–54]), and only relies on the generic fact that thermorefringent noise is correlated between the two orthogonal polarizations.

The rest of the paper is organized as follows. In Sec. I A we briefly state the main results of the paper. Section II expounds the general formalism that models the propagation of classical electromagnetic waves through a thermally-active anisotropic medium. In Sec. III A we extract stochastic equations of motion for the polarization components of the field, which are then applied to the study of propagation through an anisotropic material (Sec. III B), reflection from a crystalline thin-film coating stack (Sec. III C), and finally, reveal the existence of thermodynamically-induced beam pointing noise (Sec. III D). In Sec. IV we describe the manifestation of thermorefringent noise in quantities that are typically measured in optical experiments. Finally, in Sec. IV C we address the possibility of coherent cancellation of thermorefringent noise using balanced homodyne polarimetry.

A. Summary of main results

We establish a general formalism that describes any optical instruments affected by thermodynamic noise, in particular, generalizing all previous treatments that neglected the polarization degree of freedom [4,5,16,26,30–34]. Employing this formalism, we produce concrete predictions for thermorefringent noise in two optical configurations directly relevant to today’s most precise optical instruments—gravitational-wave detectors, optical atomic clocks—and a host of precision polarimetry experiments [44–46,55–58]. These configurations are the transmission of a plane-polarized electric field through an anisotropic medium (Sec. III B), and the reflection of a plane-polarized electric field from a periodic quarter-wavelength stack of alternating anisotropic thin-films (Sec. III C).

The incident field is taken to propagate along the z direction, and plane-polarized along the x direction, meeting the medium at normal incidence. The medium is

characterized by the dielectric tensor ϵ_{ij} , whose variation with temperature T is denoted $\epsilon'_{ij} = \partial\epsilon_{ij}/\partial T$. The medium is also assumed thermally anisotropic, with a thermal diffusion tensor D_{ij} . In equilibrium, the local temperature fluctuates with a characteristic intensity $\zeta^2 = 2k_B T^2/c_V$, where c_V is the volumetric heat capacity at constant volume.

Purely x -polarized light incident on a crystalline slab emerges with a fluctuations in its incident polarization, and additional fluctuations in the y direction. At “small” Fourier frequency Ω , we show that the polarization fluctuations along the two directions are given by (in terms of their power spectral densities of the fluctuations of the polarization component e_i along the i direction),

$$S_{e_x e_x}(\Omega) = -\frac{k^2 \zeta^2 |\epsilon'_{xx}|^2 \ell}{16\pi n_x^2 \sqrt{D_{yy} D_{xx}}} \ln(|\Omega \tau_+|)$$

$$S_{e_y e_y}(\Omega) = -\frac{k^2 \zeta^2 |\epsilon'_{xy}|^2 \ell}{16\pi n_y^2 \sqrt{D_{yy} D_{xx}}} \ln[|D_{zz} \tau_+ (k \Delta n)^2|],$$

where ℓ is the slab thickness, $k = \omega/c$ is the magnitude of the incident wave vector, $\tau_+ = (r_0^2/2)(D_{xx}^{-1} + D_{yy}^{-1})$ is the transverse thermal diffusion timescale, r_0 is the incident field’s transverse spatial mode radius, and $\Delta n = n_x - n_y$ is the static birefringence, with $n_{x,y}$ the static refractive indices in the transverse directions. Here, “small” means that $\Omega \tau_+ \ll D_{zz} \tau_+ \omega^2 (\Delta n)^2 / c^2 \ll 1$; i.e., small compared to thermal diffusion in the transverse direction (but not small compared to diffusion in longitudinal direction). Note that $S_{e_y e_y}$ is frequency-independent. In the “intermediate” frequency regime, i.e., $D_{zz} \tau_+ \omega^2 (\Delta n)^2 / c^2 \ll \Omega \tau_+ \ll 1$, $S_{e_x e_x}$ is identical to the above expression, while

$$S_{e_y e_y}(\Omega) = -\frac{k^2 \zeta^2 |\epsilon'_{xy}|^2 \ell}{16\pi n_y^2 \sqrt{D_{yy} D_{xx}}} \ln(|\Omega \tau_+|)$$

falls logarithmically. Finally, there is the “large” frequency regime, characterized by $D_{zz} \tau_+ \omega^2 (\Delta n)^2 / c^2 \ll \Omega \tau_+$ and $1 \ll \Omega \tau_+$, in which

$$S_{e_x e_x}(\Omega) = \frac{k^2 \zeta^2 |\epsilon'_{xx}|^2 \ell \tau_+}{8\pi n_x^2 r_0^2} \frac{1}{|\Omega \tau_+|^2}$$

$$S_{e_y e_y}(\Omega) = \frac{k^2 \zeta^2 |\epsilon'_{xy}|^2 \ell \tau_+}{8\pi n_y^2 r_0^2} \frac{1}{|\Omega \tau_+|^2};$$

i.e., polarization noise falls as inverse square of the frequency. Note that the polarization fluctuations in the two directions are always correlated, a detail that is discussed in Sec. III B.

We then consider the question of thermorefringent noise from a high-reflector crystalline coating stack. We model the coating as a periodic stack of a pair of

quarter-wavelength crystalline thin-films of dielectric tensors $\epsilon_{ij}^{(1,2)}$ (and approximately similar thermal properties, on a substrate that is also thermally similar). When purely x -polarized light is incident on such a stack, the polarization fluctuations of the reflected field are given by

$$S_{e_x e_x}^r(\Omega) = \left| r_x \frac{\pi n_2 \epsilon_{xx}'^{(1)} + n_1 \epsilon_{xx}'^{(2)}}{2 n_1 n_2 (n_1^2 - n_2^2)} \right|^2 S_{\bar{u} \bar{u}}(\Omega)$$

$$S_{e_y e_y}^r(\Omega) = \left| r_y \frac{\pi n_2 \epsilon_{xy}'^{(1)} + n_1 \epsilon_{xy}'^{(2)}}{2 n_1 n_2 (n_1^2 - n_2^2)} \right|^2 S_{\bar{u} \bar{u}}(\Omega),$$

where $r_{x,y}$ is the reflection amplitude for either polarization, $n_i \approx n_{ix} \approx n_{iy}$, ($i = 1, 2$) the static refractive index of each coating layer, and

$$S_{\bar{u} \bar{u}}(\Omega) \approx \frac{\zeta^2}{\pi r_0^2 \sqrt{2 D_{zz}} \Omega}$$

is the approximate power spectral density of a temperature averaged over an optically active region (in the “high”-frequency regime, $\Omega \gg D_{zz}/r_0^2$). Exact expressions for the temperature fluctuations (including in other regimes), cross-correlation between the polarizations, and the fate of the transmitted field, are all available in Sec. III C.

In the limit of isotropic thermal and optical response, the above expressions for the polarization fluctuations along the incident polarization can be related to known expressions for thermo-optic noise in an isotropic material [4,5,16,26].

II. THEORETICAL MODEL AND FORMALISM

A. Thermodynamic fluctuations in an anisotropic body

For a body in thermal equilibrium—described by the canonical ensemble—its energy fluctuates with a variance [59] $\text{Var}[E] = k_B T^2 C_V$, where T is the equilibrium temperature, and C_V the heat capacity at constant volume. The energy fluctuations may be referred to an apparent temperature fluctuation using the relation $\delta T = \delta E / C_V$ to give

$$\text{Var}[T] = \frac{k_B T^2}{C_V}. \quad (2.1)$$

We model the temperature fluctuation of the body as the spatial average of a local temperature field $u(\mathbf{r}, t)$,

$$\delta T = \frac{1}{V} \int_V u(\mathbf{r}, t) d^3 \mathbf{r}, \quad (2.2)$$

which is itself determined by a stochastic partial differential equation describing the transport of local heat fluctuations in the body. Assuming that heat transport in the body is due to conduction, the local heat current \dot{q}_i (along the i^{th} direction) is due to temperature gradients, and local temperature u decreases by heat dissipation. This is modeled by

$$\dot{q}_i = -\kappa_{ij} \partial_j u - \zeta_i(\mathbf{r}, t)$$

$$\dot{u} = -\frac{\partial_i \dot{q}_i}{c_P}, \quad (2.3)$$

where κ_{ij} is the anisotropic conductivity, c_P is the volumetric heat capacity at constant pressure, and ζ_i are stochastic heat currents modeling microscopic heat sources. Since we are interested in spatial regions larger than the typical extent of the microscopic heat sources modeled by ζ_i , and in time durations much slower than their typical fluctuation time scale, we take that they are uncorrelated in space and time [60]. However directional correlation needs to be determined separately. We consider this problem in Appendix A and conclude that the correlation of noise should take the form

$$\langle \zeta_i(\mathbf{r}, t) \rangle = 0$$

$$\langle \zeta_i(\mathbf{r}, t) \zeta_j(\mathbf{r}', t') \rangle = \zeta^2 D_{ij} \delta(\mathbf{r} - \mathbf{r}') \delta(t - t'), \quad (2.4)$$

where $D_{ij} = \kappa_{ij} / c_P$ is the thermal diffusivity. The intensity ζ^2 , determined so as to be consistent with Eq. (2.1), is (see Appendix A)

$$\zeta^2 = \frac{2k_B T^2}{c_V}, \quad (2.5)$$

where $c_V = C_V / V$ is the volumetric heat capacity at constant volume. Eliminating the heat current from Eq. (2.3) produces a stochastic partial differential equation for the temperature,

$$(\partial_t - D_{ij} \partial_i \partial_j) u(\mathbf{r}, t) = \eta(\mathbf{r}, t), \quad (2.6)$$

where $\eta = \partial_i \zeta_i$. Its formal solution,

$$u(\mathbf{r}, t) = \langle u(\mathbf{r}, t) \rangle + \int d^3 \mathbf{r}' dt' U(\mathbf{r} - \mathbf{r}', t - t') \eta(\mathbf{r}', t'), \quad (2.7)$$

is the sum of a homogeneous part $\langle u \rangle$, satisfying $(\partial_t - D_{ij} \partial_i \partial_j) \langle u \rangle = 0$, and a particular part, expressed in terms of the Green function U of the operator $(\partial_t - D_{ij} \partial_i \partial_j)$ for appropriate boundary conditions. This sum is physically interpreted as the average temperature field $\langle u \rangle$ perturbed by the fluctuation

$$\delta u(\mathbf{r}, t) \equiv \int d^3 \mathbf{r}' dt' U(\mathbf{r} - \mathbf{r}', t - t') \eta(\mathbf{r}', t'). \quad (2.8)$$

Note that since we expect $\langle u \rangle$ to be smooth, we can take D_{ij} to be symmetric.

B. Equations for electromagnetic field fluctuations

Electromagnetic wave propagation through an anisotropic medium, whose internal temperature fluctuates as

described above, is our primary concern. The predominant effect of temperature fluctuations in such a medium is a change in the relative dielectric tensor,

$$\varepsilon_{ij} = \langle \varepsilon_{ij} \rangle + \varepsilon'_{ij} \delta u. \quad (2.9)$$

Here, the coefficient ε'_{ij} may describe a temperature-dependent refractive index (along any direction), or the effect of temperature-dependent elastic strains which, via the photo-elastic effect, produces an apparent refractive index change (see Appendix B). In amorphous optical media the former (latter) leads to thermorefractive [4] (thermoelastic [26]) noise. (Note that in principle, there is also a photothermorefractive and photothermoelastic effect—i.e., the local temperature fluctuation in the medium is seeded by absorption of the local optical intensity—but these effects are usually negligible in large optics.) Restricting attention to electromagnetic field fluctuations due to temperature fluctuations that are much slower than typical optical frequencies, the field is adiabatic with respect to the fluctuations in ε_{ij} . The field then satisfies the Maxwell equations,

$$\partial_i \partial_j E_j - \partial_j \partial_j E_i = -\frac{\varepsilon_{ij}}{c^2} \partial_i^2 E_j. \quad (2.10)$$

Separating the fluctuation-free part of the field, i.e., $E_i = \langle E_i \rangle + \delta E_i$, inserting Eq. (2.9), and linearizing gives the equation for the fluctuating part of the field,

$$\partial_i \partial_j \delta E_j - \partial_j \partial_j \delta E_i + \frac{\langle \varepsilon_{ij} \rangle}{c^2} \partial_i^2 \delta E_j = -\frac{\varepsilon'_{ij} \partial_i^2 \langle E_j \rangle}{c^2} \delta u, \quad (2.11)$$

which describes electric field fluctuations driven by local temperature fluctuations.

In the typical scenario of interest, the field, in the absence of temperature fluctuations, propagates along (say) the z direction, in a pure polarization state, and in a well-characterized spatial mode $f_0(x, y)$. That is,

$$\langle E_i(\mathbf{r}, t) \rangle = \sqrt{P} e^{i(kn_z z - \omega t)} f_0(x, y) \langle e_i^{(0)} \rangle; \quad (2.12)$$

here $\langle e_i^{(0)} \rangle$ is a vector in the (x, y) plane that denotes the mean polarization state; the spatial mode is normalized such that the integral of $E_i^* E_i$ in the transverse plane gives the optical power P , i.e., $\langle e_i^{(0)} \rangle$ is a unit vector, and $|f_0|^2$ integrates to unity in the xy plane. We will only consider mean incident polarization $\langle e_i^{(0)} \rangle$ that is collinear with the principal crystal axes (i.e., the eigenvectors of $\langle \varepsilon_{ij} \rangle$). Fixing a spatial mode bases $\{f_\alpha\}_{\alpha=0,1,\dots}$ that is orthonormal under the inner product,

$$(f_\alpha | f_{\alpha'}) \equiv \int dx dy f_\alpha^*(x, y) f_{\alpha'}(x, y),$$

the effect of fluctuations in the medium can be studied by using the ansatz

$$\delta E_i(\mathbf{r}, t) = \sqrt{P} e^{i(kn_z z - \omega t)} \sum_\alpha f_\alpha(x, y) \delta e_i^{(\alpha)}(z, t) \quad (2.13)$$

that separates out the effect of the thermal fluctuation as a slow-in-time fluctuation of the polarization of the same spatial mode ($\alpha = 0$), and allows the possibility of scattering into other orthogonal modes ($\alpha \neq 0$). The latter effect must also exist in amorphous media that exhibit thermo-optic noise, and must manifest as an apparent beam pointing noise; however the theoretical formalism [61,62] used to study thermo-optic noise does not directly illuminate this possibility since it focuses on a specific observable *a priori*.

Note that the ansatz in Eq. (2.13), when restricted to the same spatial mode f as that of the mean field, i.e., $E_i = \sqrt{P} e^{i(kn_z z - \omega t)} f_0(x, y) [\langle e_i^{(0)} \rangle + \delta e_i^{(0)}]$, describes both a variation in length and angle of the polarization vector. When averaged over the ensemble of thermal fluctuations that cause these polarization fluctuations, the ansatz represents a depolarized state of light.

III. DEPOLARIZATION FROM THERMOREFRINGENT NOISE

We now turn to the study of the various manifestations of thermorefringent noise and the resulting depolarization of light. In Sec. III A we derive the equations of motion for the polarization fluctuations, which are solved in Sec. III B to estimate thermorefringent noise for transmission through a bulk crystalline optic, while in Sec. III C they are solved to estimate thermorefringent noise for reflection from a crystalline thin-film Bragg stack. Section III D briefly addresses the question of scattering noise due to thermodynamic fluctuations.

A. Equations of motion for the polarization fluctuations

We begin by restricting attention to the case where thermal fluctuations lead to polarization fluctuations of the same optical mode as the one that illuminates the medium of interest. We therefore neglect the terms proportional to the orthogonal modes $f_{\alpha \neq 0}$, then insert Eqs. (2.12) and (2.13) into Eq. (2.11), and project out the components corresponding to the spatial mode of interest f_0 . Details of this calculation are given in Appendix C. The result are the coupled equations of motion for the polarization vectors of the mode of interest,

$$\begin{aligned} \left(\frac{\partial}{\partial z} + \frac{n_x}{c} \frac{\partial}{\partial t} \right) \delta e_x^{(0)} &= \frac{ik\varepsilon'_{xx}}{2n_x} (f_0^2 | \delta u) \langle e_x^{(0)} \rangle \\ \left(\frac{\partial}{\partial z} + \frac{n_y}{c} \frac{\partial}{\partial t} \right) \delta e_y^{(0)} &= \frac{ik\varepsilon'_{xy} e^{i(n_x - n_y)kz}}{2n_y} (f_0^2 | \delta u) \langle e_x^{(0)} \rangle. \end{aligned} \quad (3.1)$$

where $n_i^2 = \epsilon_{ij}\delta_{ij}$ is the square of the refractive index along each direction, and $k = \omega/c$ is the in-vacuum wave vector. In order to obtain these equations we assume adiabatic spatial variation of the transverse mode (with respect to the spatial variation in the longitudinal direction)—which is the paraxial approximation, valid for a Gaussian spatial mode—and adiabatic temporal variation of the noise (with respect to the timescale of the optical frequency). The right hand sides of Eq. (3.1) indicate that it is precisely the spatial intensity profile of the optical field ($\propto f_0^2$) that samples the local temperature fluctuation field (δu); an aspect that is tacitly assumed in the conventional treatment [61,62], but which we derive here from first principles.

B. Polarization noise in transmission through a “thick” medium

We now consider a problem potentially relevant to any experiment where light has to traverse a crystalline material. For example, the beam-splitters and input mirrors of interferometers consisting of crystalline coatings. The main feature implicated by our theory is depolarization of the transmitted beam, which is also crucial for any precision polarimetry experiment [45,46,55–58].

We consider a crystalline material of rectangular shape, with faces separated by a distance ℓ , with normals along the z direction. The material is also assumed to be homogeneous in the sense that $\langle \epsilon_{ij} \rangle$ is constant at all spatial points. Light is incident perpendicular to one of the faces, with its incoming polarization aligned along one of the principal axis of $\langle \epsilon_{ij} \rangle$, which we take to be linearly polarized along x (without loss of generality). This can be done precisely because we have assumed $\langle \epsilon_{ij} \rangle$ is homogeneous; in fact, this also allows us to assume that $\langle \epsilon_{ij} \rangle$ is diagonal. We assume that the transverse extent of the material is infinitely large compared to the optical spot size and the thermal diffusion length. Therefore, each point of the crystal can be described by three coordinates (x, y, z) where $x, y \in (-\infty, \infty)$, and, $z \in (0, \ell)$.

The equations of motion for the polarization fluctuations [Eq. (3.1)] can then be formally solved. Since they are first order hyperbolic partial differential equations, they can be solved along the characteristics defined by $z \pm ct/n$ [[63] Sec. 11.1]. The solutions are

$$\delta e_x^{(0)}(z, t) = i \frac{k \epsilon'_{xx}}{2n_x} \langle e_x^{(0)} \rangle \int_0^z dz' F_x(z, z', t) \quad (3.2)$$

$$\delta e_y^{(0)}(z, t) = i \frac{k \epsilon'_{xy}}{2n_y} \langle e_x^{(0)} \rangle \int_0^z dz' e^{i(n_x - n_y)kz'} F_y(z, z', t), \quad (3.3)$$

where we define

$$F_i(z, z', t) = \left(f_0^2(x, y) \delta u \left(x, y, z', t + \frac{n_i}{c}(z - z') \right) \right), \quad (3.4)$$

which is the projection of the local temperature field on the optical intensity profile.

In order to complete the solution we need the fluctuating local temperature field δu . The relevant anisotropic heat equation [Eq. (2.6)] is augmented by open boundary conditions at the crystal faces. We account for these boundary conditions via the method of images [[63], Sec. 12.1]: the problem with the open boundary conditions at $z = 0, \ell$ is equivalent to the problem in all of space, but with sources placed periodically and symmetric under a mirror transformation around each of two faces. This equivalence allows us to simplify the problem by using the well-known Green’s function of the heat operator in unbounded space (a generalization of well-known results [[64], Sec. 7.4]),

$$U(\mathbf{r}, t) = [(8\pi|t|)^{3/2}(\det \mathbf{D})^{1/2}]^{-1} \exp \left[\frac{-r_i D_{ij}^{-1} r_j}{4|t|} \right]$$

and modifying the source η (rather than determining the Green’s function for the confined slab geometry while retaining the internal sources). That is, identical sources are assumed at locations $\mathbf{r}' = \pm \mathbf{r} + 2m\boldsymbol{\ell}$, where \mathbf{r} is a location of original source, $m \in \mathbb{Z}$, and $\boldsymbol{\ell} = (0, 0, \ell)$ is an ℓ -length vector along the z direction; this results in the modified source correlator,

$$\langle \eta(\mathbf{r}, t) \eta(\mathbf{r}', t') \rangle = \zeta^2 D_{ij} \partial_i \partial_j \sum_{\mathbf{s}(\mathbf{r}') \in S} \delta(\mathbf{r} - \mathbf{s}(\mathbf{r}')) \delta(t - t'), \quad (3.5)$$

where $S = \{\mathbf{s}(\mathbf{r}') = \pm \mathbf{r}' + 2m\boldsymbol{\ell}\}$. Using the Green’s function, we can then write down the correlator of the temperature field,

$$\langle \delta u(\mathbf{r}, t) \delta u(\mathbf{r}', t') \rangle = \frac{\zeta^2}{2} \sum_{\mathbf{s}(\mathbf{r}') \in S} U(\mathbf{r} - \mathbf{s}(\mathbf{r}'), t - t'), \quad (3.6)$$

which is essentially a sum of correlators of temperatures from each source point; here \mathbf{D} is the matrix form of the diffusivity tensor. To complete the formal solution of the polarization in Eqs. (3.2) and (3.3) we finally need the correlators of the source terms F_i , the projection of the temperature field on the optical intensity profile. Assuming a Gaussian transverse field profile, i.e., $f_0(x, y) = \exp[-(x^2 + y^2)/(2r_0^2)]/\sqrt{\pi r_0^2}$, we compute,

$$\langle F_i^*(z'', z, t) F_j(z''', z', t + \tau) \rangle = \frac{\zeta^2 \sum_{\mathbf{s}(\mathbf{r}') \in S} \exp[-\frac{(z-s'_z(\mathbf{r}'))^2}{4D_{zz}|\tau_{ij}|}]}{8\pi^{3/2} [D_{zz}|\tau_{ij}|(2D_{xx}|\tau_{ij}| + r_0^2)(2D_{yy}|\tau_{ij}| + r_0^2)]^{1/2}}, \quad (3.7)$$

where $\tau_{ij} = \tau + n_j(z''' - z')/c - n_i(z'' - z)/c$.

Ultimately what is observed in an experiment are signals from photodetectors impinged by fields emanating from the medium. We consider the various modes of detection more fully in Sec. IV, but the crux is that, when the optical field incident on the medium has a large mean component $\langle E_i \rangle$, the observables derived from photodetection of the emanating field are linear in the field fluctuations δE_i . In particular, since in our model the thermodynamic source noise is Gaussian, and its transduction to optical field fluctuations is linear, the statistical properties of the field fluctuations are fully characterized by its spectral covariance matrix consisting of the elements ($i, j = x, y$),

$$S_{E_i^{(0)} E_j^{(0)}}(\Omega) \equiv \int_{-\infty}^{+\infty} d\tau \langle \delta E_i^{(0)*}(\ell, t) \delta E_j^{(0)}(\ell, t + \tau) \rangle e^{-i\Omega\tau}, \quad (3.8)$$

where $\delta E_i^{(\alpha)} = (f_\alpha | \delta E_i)$, and assume that the detector is placed immediately at the exit of the crystalline slab (which is the position at which the transmitted beam is minimally depolarized [65]). Expressing the electric field fluctuation in terms of the polarization fluctuations [Eq. (2.11)], and noting that the spatial mode functions $\{f_\alpha\}$ are orthonormal, we have that,

$$S_{E_i^{(0)} E_j^{(0)}}(\Omega) = P e^{ik(n_i - n_j)\ell} S_{e_i^{(0)} e_j^{(0)}}(\omega + \Omega), \quad (3.9)$$

where $S_{e_i^{(0)} e_j^{(0)}}(\omega + \Omega)$ are the elements of the spectral covariance matrix of the polarization fluctuations, at a frequency Ω offset from the optical carrier at ω . Thus, the statistical properties of the optical field that are observable through photodetection are fully characterized by the covariance matrix of the polarization fluctuations at offset frequencies around the carrier.

In principle, Eqs. (3.2)–(3.4) and (3.7) contain the ingredients to compute the elements of this covariance matrix exactly. Below we consider a few physically interesting cases. We will exhibit the result for a crystal which is thicker than the characteristic temperature diffusion length, i.e., $\ell \gg \sqrt{D_{zz}/\Omega}$, which is valid for large optics at room temperature. Effectively, this approximation allows us to neglect fluctuating heat sources outside the interval $z \in [0, \ell]$, assume that outside this range the Gaussian function f is zero, and so extend the integration limits to $z \in [-\infty, \infty]$ for the sources that are away from the crystal surface. In this fashion, we arrive at (and dropping the superscript spatial-mode index),

$$S_{e_x e_x}(\Omega) = \frac{\zeta^2 k^2 |\epsilon'_{xx}|^2 \ell}{16\pi n_x^2 \sqrt{D_{yy} D_{xx}}} I(\Omega, n_x \Omega), \quad (3.10)$$

$$S_{e_y e_y}(\Omega) = \frac{\zeta^2 k^2 |\epsilon'_{yy}|^2 \ell}{16\pi n_y^2 \sqrt{D_{xx} D_{yy}}} I(\Omega, \omega \Delta n + n_y \Omega), \quad (3.11)$$

$$S_{e_x e_y}(\Omega) = \frac{\zeta^2 k^2 \epsilon'_{xx} \epsilon'_{yy} \ell}{16\pi n_x n_y \sqrt{D_{yy} D_{xx}}} I(\Omega, \Delta n(\omega - \Omega)) \times \frac{e^{i\omega\ell\Delta n/c} - e^{i\Omega\ell\Delta n/c}}{\Delta n(\Omega + \omega)\ell/c}, \quad (3.12)$$

where $\Delta n = n_x - n_y$, and $I(\Omega_1, \Omega_2)$ is

$$I(\Omega_1, \Omega_2) = \int_0^\infty d\tau \frac{\cos \Omega_1 \tau \exp[-\frac{\Omega_2^2}{c^2} D_{zz} \tau]}{\sqrt{(\tau + \tau_x)(\tau + \tau_y)}}. \quad (3.13)$$

Here, $\tau_{x,y}$ are the characteristic diffusion times in the transverse direction of the optical field, $\tau_{x,y} = r_0^2/2D_{xx,yy}$.

Figure 1 shows the power spectral densities Eqs. (3.10)–(3.12) as applied to two different crystal systems, crystalline silicon and lithium niobate, both for a wavelength $\lambda = 2\pi c/\omega = 1550$ nm and a beam size $r_0 = 100$ μm . The material parameters are given in Table I (Appendix B). At low frequencies, below the thermal diffusion time-scale, the fluctuations in the projection of the polarization along the direction of the incident polarization (i.e., $S_{e_x e_x}$) assumes a logarithmic form, turning over into a Ω^{-2} fall off. For materials for which the static birefringence is very small ($\Delta n \ll 1$), such as crystalline silicon (Fig. 1(a)), fluctuations in the other polarization, and the correlation between the fluctuations in either direction, also assume identical forms. For optical materials for which the static birefringence can be large ($\Delta n \lesssim 1$), such as lithium niobate (Fig. 1(b)), polarization fluctuations along the direction orthogonal to that of the incident polarization are strongly suppressed. Both types of behavior are predicted by asymptotic forms of Eqs. (3.10)–(3.12) (see Appendix D).

It is known that if an optical standing wave is formed between the faces of a bulk amorphous medium, the resulting intensity pattern changes the thermo-optic noise at frequencies $\Omega \sim 8kD_{zz}/r_0$ [76]. This effect is especially relevant in the input mirrors of Fabry-Perot cavities, which cannot be wedged to avoid a standing wave in the mirror substrate. Our formalism for the traveling wave case can be adapted to tackle the standing wave scenario. To wit, the field

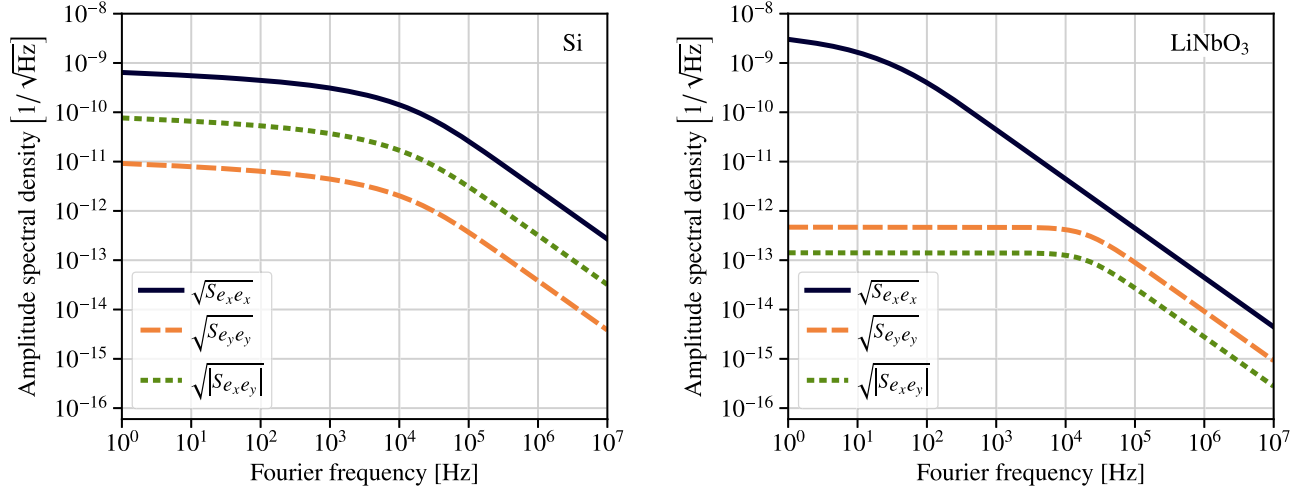


FIG. 1. Thermorefringent noise for cryogenic silicon (left) and room-temperature lithium niobate (right), using Eqs. (3.10)–(3.12). In both cases the wavelength is 1550 nm, the beam size is $r_0 = 100 \mu\text{m}$, and the material length is $\ell = 1 \text{ cm}$.

$$\langle \mathfrak{E}_i \rangle = \frac{1}{2} (\langle E_i(k) \rangle + \langle E_i(-k) \rangle) \quad (3.14)$$

represents a standing wave \mathfrak{E} as a superposition of two waves traveling in opposite directions. It then follows that the noise in the standing wave case is

$$S_{\mathfrak{E}_i^{(0)} \mathfrak{E}_j^{(0)}}(\Omega) = \frac{1}{2} S_{E_i^{(0)} E_j^{(0)}}(\Omega) + \frac{1}{2} \text{Re} \left[S_{E_i^{(0)}(-k) E_j^{(0)}(k)} \right]. \quad (3.15)$$

Here we have used the fact that the noise in polarization $E_i(-k)$ can be obtained from that in $E_i(k)$ by changing the sign of k in Eqs. (3.2) and (3.3), and sign of $z - z'$ in Eq. (3.4).

C. Polarization noise in reflection from “thin” coatings

A standard component of contemporary precision optical instruments are low-loss mirrors composed of a stack of thin films of alternating refractive index contrast [77]. Their primary mode of operation is in reflection, in which case the optical field samples a thin film stack no more than a few tens of wavelengths deep. The coating stack is made from an alternating pair of crystalline thin films (see Fig. 2) of dielectric tensors $\epsilon^{(I)}$ ($I = 1, 2$, see Fig. 2). We assume that the mirror is made in a way that the eigenvectors of their mean dielectric tensors $\langle \epsilon_{ij}^{(1,2)} \rangle$ lie in the plane transverse to the optical axis (the latter the z axis, as before). This is true of all crystalline coatings currently being fabricated. The stack is designed to produce constructive interference in reflection.

Consequently the optical field samples the coating stack no more than a few tens of wavelengths deep. Thus the relevant temperature fluctuation is that averaged over the characteristic volume occupied by the optical field, i.e.,

$$\delta \tilde{u}(t) \equiv \int_{-\infty}^{+\infty} dx dy \int_0^{+\infty} \frac{dz}{\ell_p} f_0^2(x, y) e^{-z/\ell_p} \delta u(\mathbf{r}, t); \quad (3.16)$$

here $f_0^2(x, y)$ is the transverse optical intensity profile and ℓ_p is the longitudinal penetration depth. The two materials forming the coating are described by dielectric tensors $\epsilon_{ij}^{(I)}$ ($I = 1, 2$ denotes the two materials), which are affected by the temperature according to

$$\begin{aligned} \epsilon_{ij}^{(I)}(t) &= \langle \epsilon_{ij}^{(I)} \rangle + \epsilon_{ij}^{\prime(I)} \delta \tilde{u}(t) \\ &= \begin{bmatrix} \langle [n_x^{(I)}]^2 \rangle & 0 \\ 0 & \langle [n_y^{(I)}]^2 \rangle \end{bmatrix} + \begin{bmatrix} \epsilon_{xx}^{\prime(I)} & \epsilon_{xy}^{\prime(I)} \\ \epsilon_{yx}^{\prime(I)} & \epsilon_{yy}^{\prime(I)} \end{bmatrix} \delta \tilde{u}, \end{aligned} \quad (3.17)$$

This relation suggests that to first order in $\delta \tilde{u}$ the refractive indices in the two transverse directions are

$$n_i^{(I)} \approx \langle n_i^{(I)} \rangle + \frac{\epsilon_{ii}^{\prime(I)}}{2 \langle n_i^{(I)} \rangle} \delta \tilde{u}. \quad (3.18)$$

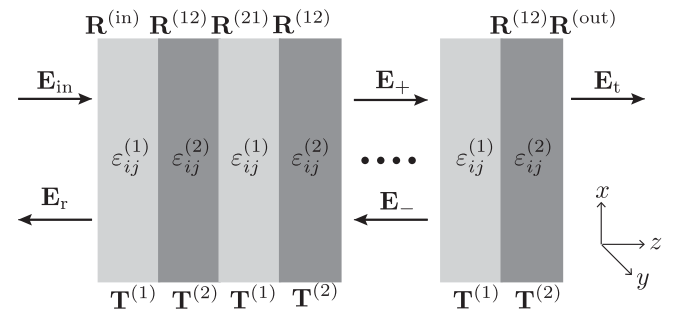


FIG. 2. Schematic picture of the mirror layers that shows the elements that correspond to propagation matrices and direction of relevant field modes.

We assume for simplicity that the incident light is pure-polarized along the x axis (and that the mirror satisfies quarter-wave stack condition for this polarization). Its polarization eigenvectors rotate by an angle

$$\delta\theta^{(I)} \approx \frac{\varepsilon_{xy}^{(I)} \delta\tilde{u}}{\langle [n_x^{(I)}]^2 \rangle - \langle [n_y^{(I)}]^2 \rangle} \quad (3.19)$$

while retaining their length. (Note that these expansions are valid as long as $|\varepsilon_{xy}' \delta\tilde{u}| \ll |n_x - n_y|$.)

1. Field propagation in a thin anisotropic coating stack

In a “thin” material, optical field propagation can be described in a scattering matrix formalism (and does not require solving the Maxwell equation as in the “thick” scenario of Sec. III B). Further simplifications arise in the periodic geometry of a coating stack. Each unit cell of the stack is composed of a pair of crystalline films of contrasting index, separated by an interface at which the index jumps (see Fig. 2). Each of the constituent films in that cell can be described by four fields assembled into a vector: $\tilde{\mathbf{E}}^{(I)} = \mathbf{E}_x^{(I)} \oplus \mathbf{E}_y^{(I)} = [E_{x+}^{(I)}, E_{x-}^{(I)}, E_{y+}^{(I)}, E_{y-}^{(I)}]^T$, where x and y denote transverse components of the field, and $+$ and $-$ denote propagation along positive and negative z axis respectively. We will denote the material to the left (right) in the unit cell by $I = 1$ ($I = 2$). Note that the way we defined the field vector implies a definition of scattering matrices different from the common definition in optics [78]. In our case the matrix that describes a system acts on the fields to the right of the system and returns fields to the left. (The common definition acts on the vector of incident fields and returns the vector of outgoing fields.) The propagation matrix that describes the passage of the field in the bulk of material I can be written in the block-diagonal form $\mathbf{T}^{(I)} = \mathbf{T}_x^{(I)} \oplus \mathbf{T}_y^{(I)}$, where $\mathbf{T}_i^{(I)} = \text{diag}[e^{-in_i^{(I)}kz}, e^{in_i^{(I)}kz}]$. At the interface between two adjacent films, the fields are described by the boundary conditions [79]

$$\mathbf{E}_+^{(1)} + \mathbf{E}_-^{(1)} = \mathbf{E}_+^{(2)} + \mathbf{E}_-^{(2)}, \quad (3.20)$$

$$\mathbf{B}_+^{(1)} + \mathbf{B}_-^{(1)} = \mathbf{B}_+^{(2)} + \mathbf{B}_-^{(2)}, \quad (3.21)$$

for the electric and magnetic fields. Note that the electric and magnetic fields are related through; $cB_x = -n_y E_y$, $cB_y = n_x E_x$. To write the correct matrix that describes transfer at the interface, we need to account for the relative rotation of the eigenvectors of the dielectric tensor between adjacent layers. Since it is convenient to work in the basis of eigenvectors of each material, we would like to write the interface transfer matrix in a way that it transforms the field vectors in material 2 (written in the natural basis of material 2) to field vectors in material 1 (written in its natural basis).

Employing the boundary conditions in Eqs. (3.20) and (3.21) and accounting for the rotation of the field vectors at the interface, we arrive at the transfer matrix

$$\mathbf{R}^{(12)} = \begin{bmatrix} \mathbf{r}_{xx}^{(12)} \cos \delta\theta & -\mathbf{r}_{xy}^{(12)} \sin \delta\theta \\ \mathbf{r}_{yx}^{(12)} \sin \delta\theta & \mathbf{r}_{yy}^{(12)} \cos \delta\theta \end{bmatrix}, \quad (3.22)$$

where $\mathbf{r}_{ij}^{(IJ)} \equiv \mathbf{r}(n_i^{(I)}, n_j^{(J)})$ with

$$\mathbf{r}(a, b) \equiv \frac{1}{2} \begin{bmatrix} 1 + \frac{b}{a} & 1 - \frac{b}{a} \\ 1 - \frac{b}{a} & 1 + \frac{b}{a} \end{bmatrix}, \quad (3.23)$$

and the rotation angle $\delta\theta = \delta\theta^{(2)} - \delta\theta^{(1)}$ is the difference of the thermodynamically fluctuating polarization angle described above in Eq. (3.19).

The transfer through a single unit cell—composed of material 1 followed by material 2—is given by the matrix

$$\Phi = \mathbf{R}^{(12)} \mathbf{T}^{(2)} \mathbf{R}^{(21)} \mathbf{T}^{(1)}. \quad (3.24)$$

It describes (reading right to left), propagation through material 1, transfer at the 12 interface, propagation in material 2, and transfer at the 21 interface. The matrix $\mathbf{R}^{(21)}$ is can be obtained from $\mathbf{R}^{(12)}$ by swapping all material indices (i.e., $1 \leftrightarrow 2$), and by inverting the rotation angles (i.e., $\theta \rightarrow -\theta$). Since the coating is a periodic array of such a unit cell, the transfer matrix for the coating is

$$\mathbf{M} = \mathbf{R}^{(\text{in})} \mathbf{T}^{(1)} \Phi^N \mathbf{R}^{(\text{out})}. \quad (3.25)$$

where $\mathbf{R}^{(\text{in}, \text{out})}$ are the transfer matrices for the entrance and substrate interfaces, and we have assumed (without loss of generality) that material 1 is the entrance coating.

In order to fully specify the transfer matrix \mathbf{M} we need a model of the entrance coating layer [i.e., the factor $\mathbf{R}^{(\text{in})} \mathbf{T}^{(1)}$] and the substrate [the factor $\mathbf{R}^{(\text{out})}$]. The former is given by

$$\mathbf{R}^{(\text{in})} \mathbf{T}^{(1)} \approx \begin{bmatrix} \mathbf{r}_x^{(1)} \mathbf{T}_x^{(1)} & \mathbf{r}_y^{(1)} \mathbf{T}_y^{(1)} \delta\theta^{(1)} \\ \mathbf{r}_x^{(1)} \mathbf{T}_x^{(1)} \delta\theta^{(1)} & \mathbf{r}_y^{(1)} \mathbf{T}_y^{(1)} \end{bmatrix}, \quad (3.26)$$

where, assuming the optical field enters from vacuum, $\mathbf{r}_i^{(1)} = \mathbf{r}(1, n_i^{(1)})$, and $\delta\theta^{(1)}$ is given by Eq. (3.19). The effect of the substrate is modeled by

$$\mathbf{R}_{\text{out}} \approx \begin{bmatrix} \mathbf{r}_x^{(s)} & -\mathbf{r}_y^{(s)} \delta\theta^{(1)} \\ -\mathbf{r}_x^{(s)} \delta\theta^{(1)} & \mathbf{r}_y^{(s)} \end{bmatrix}, \quad (3.27)$$

where, assuming the substrate has a refractive index n_s , $\mathbf{r}_i^{(s)} = \mathbf{r}(n_s, n_i^{(2)})$.

The thermorefringent behavior of the coating stack is encoded in the dependence of the matrix \mathbf{M} on the polarization angle fluctuation $\delta\theta$. Of this, the dominant contribution comes from the factor Φ^N ; for small angle fluctuations about zero, $\Phi \approx \langle \Phi \rangle + \Phi' \delta\theta$, so that Φ^N scales as $N\delta\theta$. (This scaling discounts the possibility of engineering the coating stack to harness correlated thermorefringent fluctuations across the coating layers, we limit attention to this case since it illustrates the state-of-the-art in crystalline coatings.) The mean unit cell transfer matrix $\langle \Phi \rangle$ turns out to be block-diagonal; $\langle \Phi \rangle = \langle \Phi_{xx} \rangle \oplus \langle \Phi_{yy} \rangle$, where $\langle \Phi_{ii} \rangle \equiv \mathbf{r}_{ii}^{(12)} \mathbf{T}_i^{(2)} \mathbf{r}_{ii}^{(21)} \mathbf{T}_i^{(1)}$. It indicates that if the incident field polarization is aligned along the eigenvectors of the mean dielectric tensor, the mean outgoing field experiences no change in polarization. The perturbation Φ' is off-diagonal,

$$\Phi' = \begin{bmatrix} 0 & \Phi_{xy} \\ \Phi_{yx} & 0 \end{bmatrix}, \quad (3.28)$$

$$\Phi_{xy} = \mathbf{r}_{xx}^{(12)} \mathbf{T}_x^{(2)} \mathbf{r}_{xy}^{(21)} \mathbf{T}_y^{(1)} - \mathbf{r}_{xy}^{(12)} \mathbf{T}_y^{(2)} \mathbf{r}_{yy}^{(21)} \mathbf{T}_y^{(1)}, \quad (3.29)$$

$$\Phi_{yx} = \mathbf{r}_{yx}^{(12)} \mathbf{T}_x^{(2)} \mathbf{r}_{xx}^{(21)} \mathbf{T}_x^{(1)} - \mathbf{r}_{yy}^{(12)} \mathbf{T}_y^{(2)} \mathbf{r}_{yx}^{(21)} \mathbf{T}_x^{(1)}, \quad (3.30)$$

describing the inscription of thermorefringent polarization fluctuations on the mean field, and the consequent conversion of a pure-polarized input field into a mixed state of polarization as it propagates through even a single unit cell of the coating.

In principle, once the mirror stack is specified, the matrices $\langle \Phi \rangle$ and Φ' can be assembled, and the statistical properties of the resulting polarization state of the field studied. If one wants to solve the analogous problem for an arbitrary stack of dielectric layers, one will need to replace

Φ^N in Eq. (3.25) with $\prod_i \Phi_i$, where Φ_i is the matrix that describes the i th pair of layers.

2. Specialization to the case of a high-reflector

Our interest here is to illustrate thermorefringent noise in a simple relevant example. Typically, the crystalline thin film stack is configured to act as a highly reflective mirror. To assure the highest reflection coefficient possible, the films must satisfy a quarter-wave condition [80]. This condition is typically chosen to be satisfied for one particular value of wave vector k , which then constrains the thickness of each film to be $\ell^{(l)} = \pi/(2kn^{(l)})$. In the following we assume that this condition is met. For typical crystalline materials used in contemporary mirrors, the in-plane optical anisotropy is small, i.e., $|\Delta n| = |n_x - n_y| \ll 1$. Thus we also assume that the refractive index along the y axis is close to that along the x axis; $n_y^{(l)} = n_x^{(l)} + \Delta n_l$, with $\Delta n_l \ll 1$. In this case, the matrices $\langle \Phi \rangle$ and Φ' can be simplified by considering their expansions to lowest order in $\Delta n^{(l)}$. Note that according to Eq. (3.18) an expansion in Δn will reproduce one in $\delta\bar{u}$.

The mirror matrix up to lowest order in $\delta\bar{u}$ can thus be written

$$\mathbf{M} = \langle \mathbf{M} \rangle + \mathbf{M}' \delta\bar{u}. \quad (3.31)$$

Here, $\langle \mathbf{M} \rangle$ captures the static birefringence of the mirror, and is given by

$$\langle \mathbf{M} \rangle = \frac{-in_1\Gamma}{2} \begin{bmatrix} 1 & 1 \\ -1 & -1 \end{bmatrix} \oplus \begin{bmatrix} 1 & 1 \\ -1 & -1 \end{bmatrix}, \quad (3.32)$$

where $\Gamma \equiv (-n_1/n_2)^N$. The matrix \mathbf{M}' captures the effect of thermorefringent noise, and is given by

$$\mathbf{M}' = \Gamma \begin{bmatrix} -\left(\frac{iNn_1}{4}\alpha_{xx} + \frac{i\epsilon_{xx}^{(1)}}{4n_1}\right)\mathbf{A} - \frac{\pi\beta_{xx}^+}{8n_2}\mathbf{A}_s & \left(\frac{iNn_1}{4}\alpha_{xy} + \frac{i\epsilon_{xy}^{(1)}}{4n_1} - \frac{iN\epsilon_{xy}^{(2)}\Delta n_2}{2n_2\Delta n_1}\right)\mathbf{A} + \left(\frac{\beta_{xy}^-}{8n_2} + \frac{\pi\epsilon_{xy}^{(1)}\Delta n_2}{4(n_1^2 - n_2^2)\Delta n_1}\right)\mathbf{A}_s \\ -\left(\frac{iNn_1}{4}\alpha_{xy} + \frac{i\epsilon_{xy}^{(1)}}{4n_1}\right)\mathbf{A} - \frac{\pi\beta_{xy}^+}{8n_2}\mathbf{A}_s & -\left(\frac{iNn_1}{4}\alpha_{yy} + \frac{i\epsilon_{yy}^{(1)}}{4n_1}\right)\mathbf{A} - \frac{\pi\beta_{yy}^+}{8n_2}\mathbf{A}_s \end{bmatrix}, \quad (3.33)$$

where we have defined

$$\mathbf{A} = \begin{bmatrix} 1 & 1 \\ -1 & -1 \end{bmatrix}, \quad \mathbf{A}_s = \begin{bmatrix} 1 + n_s & 1 - n_s \\ 1 + n_s & 1 - n_s \end{bmatrix},$$

and $\alpha_{ij} = (\epsilon_{ij}^{(1)}/n_1^2) - (\epsilon_{ij}^{(2)}/n_2^2)$, $\beta_{ij}^\pm = [n_2\epsilon_{ij}^{(1)} \pm n_1\epsilon_{ij}^{(2)}]/(n_1^2 - n_2^2)$.

Ultimately, we are interested in the optical fields transmitted through and reflected from the mirror stack. When the mirror matrix \mathbf{M} is computed, the relation between the

light in front of the mirror and behind the mirror is given by the equation

$$\begin{bmatrix} E_x^{\text{inc}} \\ E_x^{\text{r}} \\ 0 \\ E_y^{\text{r}} \end{bmatrix} = \begin{bmatrix} M_{11} & M_{12} & M_{13} & M_{14} \\ M_{21} & M_{22} & M_{23} & M_{24} \\ M_{31} & M_{32} & M_{33} & M_{34} \\ M_{41} & M_{42} & M_{43} & M_{44} \end{bmatrix} \begin{bmatrix} E_x^{\text{t}} \\ 0 \\ E_y^{\text{t}} \\ 0 \end{bmatrix}, \quad (3.34)$$

where E_x^{inc} is an incident x -polarized field, $E_{x,y}^{\text{r}}$ are the two polarizations of the reflected field, and $E_{x,y}^{\text{t}}$ are the

transmitted fields. In order to arrive at the conventional scattering description that relates the input fields (E_x^{inc}) to the output fields ($E_{x,y}^{\text{r,t}}$), the matrix \mathbf{M} needs to be permuted so as to solve the linear equations Eq. (3.34). Doing so gives the transmission and reflection coefficients of the high-reflector stack,

$$\begin{aligned} t_x &= \frac{M_{33}}{M_{11}M_{33} - M_{13}M_{31}} \\ t_y &= -\frac{M_{31}}{M_{11}M_{33} - M_{13}M_{31}} \\ r_x &= \frac{M_{21}M_{33} - M_{23}M_{31}}{M_{11}M_{33} - M_{13}M_{31}} \\ r_y &= \frac{M_{41}M_{33} - M_{43}M_{31}}{M_{11}M_{33} - M_{13}M_{31}}. \end{aligned}$$

Notice that these coefficients are stochastic through their dependence on $\delta\tilde{u}$. Although this dependence is nonlinear, when the fluctuations are small, in the sense that the fractional change in the matrix element M_{ij} due to $\delta\tilde{u}$, $\langle M_{ij}^{-1} \rangle (\partial M_{ij} / \partial \tilde{u}) \delta\tilde{u} \ll 1$, we can approximate the effect of the fluctuating temperature via a linear expansion in $\delta\tilde{u}$, even for the fields. In this fashion, we derive the fluctuating parts of the transmitted and reflected fields,

$$\begin{aligned} \delta E_x^{\text{t}} &= -\langle E_x^{\text{t}} \rangle \frac{M'_{11}}{\langle M_{11} \rangle} \delta\tilde{u} \\ \delta E_y^{\text{t}} &= -\langle E_x^{\text{t}} \rangle \frac{M'_{31}}{\langle M_{33} \rangle} \delta\tilde{u} \\ \delta E_x^{\text{r}} &= \langle E_x^{\text{r}} \rangle \left(\frac{M'_{21}}{\langle M_{21} \rangle} - \frac{M'_{11}}{\langle M_{11} \rangle} \right) \delta\tilde{u} \\ \delta E_y^{\text{r}} &= \langle E_x^{\text{r}} \rangle \left(\frac{M'_{41}}{\langle M_{21} \rangle} - \frac{\langle M_{43} \rangle M'_{31}}{\langle M_{33} \rangle \langle M_{21} \rangle} \right) \delta\tilde{u}. \end{aligned} \quad (3.35)$$

Notice that the polarization fluctuations in both transverse directions is proportional to fluctuations in the average temperature fluctuation $\delta\tilde{u}$ in the crystalline thin-film stack.

3. Spectrum of the polarization fluctuations

All that is required in order to extract the spectrum of polarization fluctuations from Eq. (3.35) is the spectrum of $\delta\tilde{u}$. The latter can be calculated from its definition [Eq. (3.16)]

$$\delta\tilde{u} = \frac{1}{\pi r_0^2 \ell_p} \int_{-\infty}^{+\infty} dx dy \int_0^{+\infty} dz \delta u(\mathbf{r}, t) e^{-(x^2+y^2)/r_0^2} e^{-z/\ell_p},$$

by employing the fluctuation-dissipation theorem for the heat source [Eq. (2.4)], and propagating it through to δu using the Green's function for the heat equation [Eq. (2.7)] in the infinite plane with open boundary conditions (we assume the beam spot size to be much smaller than the size of the optic). The resulting spectral density of the volume-averaged temperature is

$$S_{\tilde{u}\tilde{u}}(\Omega) = \int_{-\infty}^{+\infty} \frac{d^3\mathbf{K}}{(2\pi)^3} \frac{4\zeta^2 (D_{ij}K_iK_j) \exp[-\frac{(K_x^2+K_y^2)r_0^2}{2}]}{(1+K_z^2\ell_p^2)(\Omega^2+(D_{ij}K_iK_j)^2)}. \quad (3.36)$$

In the thermally isotropic case, i.e., if $K_z^2\ell_p^2 \ll 1$, this expression reduces to that of Braginsky *et al.* [4]. In the thermally anisotropic case, two relevant asymptotic forms of Eq. (3.36) are

$$S_{\tilde{u}\tilde{u}}(\Omega) = \frac{\zeta^2}{\pi r_0} \begin{cases} \frac{(2\text{Tr}\mathbf{D}_{\perp}^2)^{-\frac{1}{4}}}{\sqrt{\pi D_{zz}}} K(\sin\frac{\phi}{2}); & \Omega \ll \frac{D}{r_0} \\ \frac{1}{r_0\sqrt{2D_{zz}\Omega}}; & \Omega \gg \frac{D}{r_0}, \end{cases} \quad (3.37)$$

where

$$\mathbf{D}_{\perp} = \begin{bmatrix} D_{xx} & D_{xy} \\ D_{xy} & D_{yy} \end{bmatrix}, \quad (3.38)$$

and D is the typical diagonal element of this matrix (assumed roughly comparable), K is the complete elliptic integral of the first kind, and $\cos\phi = (\text{Tr}\mathbf{D}_{\perp})/\sqrt{2\text{Tr}\mathbf{D}_{\perp}^2}$. Note that all these results rely on the beam spot size being larger than the penetration depth (i.e., $r_0 \gg \ell_p$). Additionally, we note that in the above expressions, the appropriate material parameters to use are those of the substrate; this amounts to the statement that the temperature fluctuations near the surface of the coating are dominated by the effect of heat flow in the substrate.

Substituting Eq. (3.36) into Eq. (3.35) gives us the spectral density of the polarization fluctuations,

$$S_{e_x e_x}^{\text{t}}(\Omega) = \left| t_x \frac{N}{2} \left(\frac{\epsilon_{xx}^{\prime(1)}}{n_1^2} - \frac{\epsilon_{xx}^{\prime(2)}}{n_2^2} \right) \right|^2 S_{\tilde{u}\tilde{u}}(\Omega), \quad (3.39)$$

$$S_{e_x e_x}^{\text{r}}(\Omega) = \left| r_x \frac{\pi n_2 \epsilon_{xx}^{\prime(1)} + n_1 \epsilon_{xx}^{\prime(2)}}{2 n_1 n_2 (n_1^2 - n_2^2)} \right|^2 S_{\tilde{u}\tilde{u}}(\Omega), \quad (3.40)$$

$$S_{e_y e_y}^{\text{t}}(\Omega) = \left| t_y \frac{N}{2} \left(\frac{\epsilon_{xy}^{\prime(1)}}{n_1^2} - \frac{\epsilon_{xy}^{\prime(2)}}{n_2^2} \right) \right|^2 S_{\tilde{u}\tilde{u}}(\Omega), \quad (3.41)$$

$$S_{e_y e_y}^{\text{r}}(\Omega) = \left| r_y \frac{\pi n_2 \epsilon_{xy}^{\prime(1)} + n_1 \epsilon_{xy}^{\prime(2)}}{2 n_1 n_2 (n_1^2 - n_2^2)} \right|^2 S_{\tilde{u}\tilde{u}}(\Omega). \quad (3.42)$$

Note that cross-correlations can be computed the same way and will have the same dependence on $S_{\tilde{u}\tilde{u}}(\Omega)$. These equations are valid for any crystalline mirror Bragg stack operated near the quarter wavelength stack condition, for any crystalline material whose in-plane optical anisotropy is small (i.e., $|\Delta n| \ll 1$). They thus describe crystalline mirrors currently being considered for all precision optical instruments.

The plot for the relative power spectral density for one particular coating system (AlGaAs/GaAs) is shown in

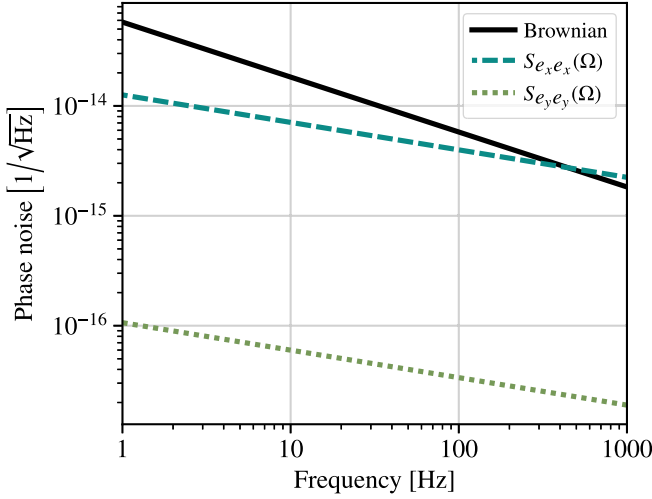


FIG. 3. Thermorefringent noise [Eqs. (3.40) and (3.42)] for an AlGaAs/GaAs high reflector of 50 quarter-wave layers, with 1500 nm light with radius $r_0 = 4$ cm. The comparison with the Brownian noise of the coating is also shown.

Fig. 3. The material parameters are given in Table I (Appendix B). Note that the estimate here depicts an alternating stack of identical AlGaAs/GaAs layers, which may not be optimal from the perspective of reducing thermorefringent noise. As in the case of amorphous coatings, where the thin-film stack structure can be optimized [32,54] to reduce thermo-optic noises, it may also be possible to optimize the stack structure of crystalline coatings to optimize thermorefringent noise. The thermo-refractive and thermorefringent noises of the coating are also compared to the Brownian noise, which has a phase noise power spectral density $S_{\text{cBr}}(\Omega) \simeq (2\pi/\lambda)^2 (4k_B T / \pi r_0^2 \Omega E) (1 - \sigma - 2\sigma^2) \phi d$ [34,51]. Here the coating thickness is $d = 6 \mu\text{m}$ and the coating loss angle is $\phi = 1 \times 10^{-5}$. The approximation symbol indicates that the effect of the light penetration into the coating has been ignored, as has the disparity in the mechanical parameters of the coating and substrate (we chose typical values of $E = 100$ GPa for the Young modulus and $\sigma = 0.2$ for the Poisson ratio).

D. Thermodynamic beam-pointing noise

The manifestations of thermodynamic noise considered so far describe the effect of thermal fluctuations in an anisotropic medium on the same spatial mode of the field as the one used to probe the medium. A qualitatively different effect is that where thermodynamic dielectric fluctuations scatter light from the spatial mode of the incident field to an orthogonal mode. If the incident field is a transverse mode that is cylindrically symmetric, and the scattering is predominantly into modes that break that cylindrical symmetry, the effect of scattering is an apparent change in the angle of the optical beam—that is, beam pointing noise of thermodynamic origin.

In this section we describe thermodynamic beam-pointing noise. A proper accounting of this effect calls for a modal resolution of the optical field [Eq. (2.13)], see also Appendix C],

$$\delta E_i(\mathbf{r}, t) = \sqrt{P} e^{i(kn_i z - \omega t)} \left\{ f_0(x, y) \delta e_i^{(0)}(z, t) + \sum_{\alpha \geq 1} f_\alpha(x, y) \delta e_i^{(\alpha)}(z, t) \right\}, \quad (3.43)$$

where the spatial mode f_0 is taken to be the one populated in the incident field, and the higher-order modes $f_{\alpha \geq 1}$ are populated by thermodynamically-induced scattering. We focus attention on a single higher-order mode to which scattering is predominant. For example, this captures the common scenario where light in a fundamental Gaussian mode of a laser ($f_0 = \exp[-(x^2 + y^2)/(2r_0^2)] / \sqrt{\pi r_0^2}$) is scattered into a (1,0) Hermite-Gauss mode ($f_1 = \sqrt{2/\pi r_0^2} x \exp[-(x^2 + y^2)/(2r_0^2)]$). Since both the modes vary much slower in the transverse direction than along the propagation direction, arguments similar to the ones in Appendix C can be employed to separate out from the Maxwell equations for the field fluctuations [Eq. (2.11)], the equations for the polarization components of the relevant higher order mode. This gives,

$$\begin{aligned} \left(\frac{\partial}{\partial z} + \frac{n_x}{c} \frac{\partial}{\partial t} \right) \delta e_x^{(1)} &= \frac{ik \epsilon'_{xx}}{2n_x} (f_1 | f_0 \delta u) \langle e_x^{(0)} \rangle \\ \left(\frac{\partial}{\partial z} + \frac{n_y}{c} \frac{\partial}{\partial t} \right) \delta e_y^{(1)} &= \frac{ik \epsilon'_{xy} e^{i(n_x - n_y) kz}}{2n_x} (f_1 | f_0 \delta u) \langle e_x^{(0)} \rangle. \end{aligned} \quad (3.44)$$

These are very similar to Eq. (3.1), except that the stochastic source term on the right-hand side involves the spatial overlap $(f_1 | f_0 \delta u)$ that describes the scattering efficiency from the fundamental mode to the higher-order mode mediated by the temperature field δu . Employing arguments and techniques similar to the ones in Sec. III B, we calculate the correlation function of the source,

$$\begin{aligned} &\langle (f_1 | f_0 \delta u(\mathbf{r}, t)) (f_1 | f_0 \delta u(\mathbf{r}', t + \tau)) \rangle \\ &= \frac{\zeta^2 r_0^2 \sum_{s \in S} \exp[-\frac{(z-s')^2}{4D_{zz}|\tau|}]}{16\sqrt{\pi^3} \sqrt{D_{zz}|\tau|} \sqrt{(2D_{xx}|\tau| + r_0^2)^3 (2D_{yy}|\tau| + r_0^2)}}. \end{aligned} \quad (3.45)$$

This fixes the statistical properties of the source that drives Eq. (3.44). Since the latter is structurally similar to the equations of motion that describe the transmission problem in Sec. III B, they can be solved similarly. We thus arrive at the spectral density of the polarization fluctuations in the higher-order mode,

$$S_{e_x^{(1)} e_x^{(1)}} = \frac{\zeta^2 k^2 |\epsilon'_{xx}|^2 \ell r_0^2}{64\pi n_x^2 \sqrt{D_{yy} D_{xx}^3}} I^{(1)}(\Omega, n_x \Omega) \quad (3.46)$$

$$S_{e_y^{(1)} e_y^{(1)}} = \frac{\zeta^2 k^2 |\epsilon'_{xy}|^2 \ell r_0^2}{64\pi n_y^2 \sqrt{D_{yy} D_{xx}^3}} I^{(1)}(\Omega, n_x \omega + n_y \Omega), \quad (3.47)$$

where

$$I^{(1)}(\Omega_1, \Omega_2) = \int_0^\infty d\tau \frac{\cos \Omega_1 \tau \exp[-\frac{\Omega_2^2}{c^2} D_{zz} \tau]}{\sqrt{(\tau + \tau_x)^3 (\tau + \tau_y)}} \quad (3.48)$$

is analogous to the integral in Eq. (3.13). For Fourier frequencies that are small compared to the thermal diffusion timescale (i.e., $D_z \tau_+ / \ell^2 \ll \Omega \tau_+ \ll 1$), the required limiting expressions for $I^{(1)}$ are given by

$$I^{(1)}(0, 0) = \frac{2}{\sqrt{\tau_x} (\sqrt{\tau_x} + \sqrt{\tau_y})}$$

$$I^{(1)}(0, n_x k c) = \frac{1}{k^2 n_x^2 D_{zz} \sqrt{\tau_x^3 \tau_y}}.$$

Using these, we have the power spectral density of the polarization fluctuations of the higher-order mode,

$$S_{e_x^{(1)} e_x^{(1)}} = \frac{\zeta^2 k^2 |\epsilon'_{xx}|^2 \ell}{32\pi n_x^2 \sqrt{D_{xx}} (\sqrt{D_{xx}} + \sqrt{D_{yy}})},$$

$$S_{e_y^{(1)} e_y^{(1)}} = \frac{\zeta^2 k^2 |\epsilon'_{xy}|^2 \ell}{32\pi n_x^2 n_y^2 D_{zz} r_0^2}, \quad (3.49)$$

which are both white noise at these low frequencies.

1. Thermodynamic pointing noise in amorphous media

The above equations predict that even for an amorphous medium, beam-pointing noise due to thermodynamically-mediated scattering into higher order modes can exist. Indeed, in general [81], scattering of light from the (0,0) Gaussian mode into the (1,0) or (0,1) Hermite-Gauss mode is equivalent to beam pointing noise by an angle $\delta\psi = (kr_0)^{-1} (f_1 |\delta E_x|) / \sqrt{P}$. Thus, the spectral density of the beam pointing angle fluctuations is given by $S_{\psi\psi} = (kr_0)^{-2} S_{e_x^{(1)} e_x^{(1)}}$. For an amorphous medium, characterized by an isotropic thermal conductivity $D_{ij} = \delta_{ij} D$ and an isotropic dielectric constant

$$\epsilon_{ij} = \delta_{ij} \left(n + \frac{\partial n}{\partial T} \right)^2 W^2 \approx \delta_{ij} \left(n^2 + 2n \frac{\partial n}{\partial T} \right),$$

where n is the (average) refractive index, Eq. (3.49) reduces to

$$S_{e_x^{(1)} e_x^{(1)}}(\Omega) = \frac{(\zeta k)^2 \ell}{16\pi D} \left(\frac{\partial n}{\partial T} \right)^2. \quad (3.50)$$

Referring these to beam pointing angle, we find

$$S_{\psi\psi}(\Omega) = \frac{\zeta^2 \ell}{16\pi r_0^2 D} \left(\frac{\partial n}{\partial T} \right)^2. \quad (3.51)$$

For the geometry considered previously ($r_0 = 100 \mu\text{m}$, $\ell = 1 \text{ cm}$), the pointing fluctuation in cryogenic silicon (Table I in Appendix B) is of order $10^{-13} \text{ rad}/\sqrt{\text{Hz}}$; for room-temperature fused silica [82] it is of order $10^{-12} \text{ rad}/\sqrt{\text{Hz}}$.

IV. MANIFESTATION OF POLARIZATION NOISE IN OPTICAL DETECTION

The previous sections establish the formalism, and then use it to determine polarization fluctuations in optical fields due to their interaction with crystalline optical materials in thermal equilibrium. The precise manner in which these polarization fluctuations manifest in signals that are typically measured in an experiment is the concern of this section.

A. Direct photodetection

We will consider, as before, that the electric field in the plane transverse to the propagation direction is of the form [Eqs. (2.12) and (2.13)], with mode indices dropped under the assumption that we limit attention to a single spatial mode; i.e., neglecting beam pointing noise]

$$E_i(\mathbf{r}, t) = \langle E_i(\mathbf{r}, t) \rangle + \delta E_i(\mathbf{r}, t), \quad (i = x, y) \quad (4.1)$$

where

$$\langle E_i \rangle = \sqrt{P} e^{i(kn_i z - \omega t)} f(x, y) \langle e_i \rangle$$

$$\delta E_i = \sqrt{P} e^{i(kn_i z - \omega t)} f(x, y) \delta e_i(z, t). \quad (4.2)$$

This field is incident on a photoemissive surface, held perpendicular to the propagation direction, at $z = \ell$. The photocurrent emitted by the detector is then [83]

$$I(t) = \alpha \int_{\mathcal{D}} d^2 \mathbf{r} E_i^*(\mathbf{r}, t) E_i(\mathbf{r}, t),$$

where α is the responsivity, \mathcal{D} is the domain of the photoemissive surface, $\mathbf{r} = (x, y, \ell)$, and $d^2 \mathbf{r} = dx dy$. We will assume that the area of \mathcal{D} is much larger than the transverse extent of the electric fields involved so that the optical beam is not clipped; we will thus extend the above integrals to the entire xy plane. Using Eq. (4.1) in the above equation, and neglecting terms second order in the electric field fluctuations, the photocurrent splits into a mean (“DC”) part and a fluctuating (“AC”) component:

$$\begin{aligned}
I(t) &\approx \langle I \rangle + \delta I(t) \\
\langle I \rangle &= \alpha \int d^2\mathbf{r} |\langle E_i \rangle|^2 \\
\delta I &= \alpha \int d^2\mathbf{r} (\langle E_i^* \rangle \delta E_i + \text{c.c.}). \quad (4.3)
\end{aligned}$$

Since δI is linear in δE_i , and the latter is a Gaussian stochastic process, so is the former. Thus the statistical properties of the photocurrent are fully characterized by the two-time correlation function, $C_{II}(t, \tau) = \langle \delta I(t) \delta I(t + \tau) \rangle$. Using the explicit form of δI , its correlation function can be written as

$$\begin{aligned}
C_{II}(t, \tau) &= \alpha^2 \int d^2\mathbf{r} d^2\mathbf{r}' \{ [\langle E_i^*(\mathbf{r}, t) \rangle \langle \delta E_i(\mathbf{r}, t) \delta E_j^*(\mathbf{r}', t + \tau) \rangle \langle E_j(\mathbf{r}', t) \rangle + \text{c.c.}] \\
&\quad + [\langle E_i^*(\mathbf{r}, t) \rangle \langle \delta E_i(\mathbf{r}, t) \delta E_j(\mathbf{r}', t + \tau) \rangle \langle E_j^*(\mathbf{r}', t) \rangle + \text{c.c.}] \}. \quad (4.4)
\end{aligned}$$

All four terms here are independent of the optical frequency ω , so that the statistical properties of the photocurrent are independent of the optical carrier. The first two terms are further only sensitive to stationary fluctuations of the field, whereas the second pair are sensitive to non-stationary fluctuations as well. We neglect the second pair of terms since field fluctuations due to thermorefringent noise are stationary. Then the correlation function only depends on the time delay τ ; so we use the notation, $C_{II}(\tau) = C_{II}(t, \tau)$. Introducing the two-point correlation function of the electric field,

$$C_{E_i E_j}(\mathbf{r}', \tau) \equiv \langle \delta E_i(\mathbf{r}, t) \delta E_j^*(\mathbf{r} + \mathbf{r}', t + \tau) \rangle \quad (4.5)$$

we have

$$\begin{aligned}
C_{II}(\tau) &= \alpha^2 \int d^2\mathbf{r} d^2\mathbf{r}' [\langle E_i^*(\mathbf{r}, t) \rangle C_{E_i E_j}(\mathbf{r} - \mathbf{r}', \tau) \\
&\quad \times \langle E_j(\mathbf{r}', t + \tau) \rangle + \text{c.c.}]. \quad (4.6)
\end{aligned}$$

Using the explicit form of the field fluctuations in Eq. (4.2), we have that,

$$C_{E_i E_j}(\mathbf{r}', \tau) = P f(\mathbf{r}) f^*(\mathbf{r} + \mathbf{r}') C_{e_i e_j}(\tau),$$

where $C_{e_i e_j}(\tau) \equiv \langle \delta e_i(\ell, t) \delta e_j^*(\ell, t + \tau) \rangle$, is the correlation function of the vectorial polarization fluctuations. Inserting the expression for the mean field from Eq. (4.2) in Eq. (4.6), the spatial integral in Eq. (4.6) factorizes out, which gives a numerical constant that can be absorbed by redefining the responsivity α (and in fact describes the geometric contribution to the detection efficiency); we thus arrive at

$$C_{II}(\tau) = (\alpha P)^2 [\langle e_i^* \rangle C_{e_i e_j}(\tau) \langle e_j \rangle + \text{c.c.}]. \quad (4.7)$$

Finally, stationary photocurrent fluctuations can be equivalently described by the Fourier transform of its two-time correlation function, the power spectral density, $S_{II}(\Omega) = \int C_{II}(\tau) e^{i\Omega\tau} d\tau$, which assumes the form,

$$S_{II}(\Omega) = (\alpha P)^2 [\langle e_i^* \rangle S_{e_i e_j}(\Omega) \langle e_j \rangle + \text{c.c.}]. \quad (4.8)$$

These photocurrent fluctuations can be referred to relative intensity noise of the optical field, $S_{II}/(\alpha P)^2 = \langle e_i^* \rangle S_{e_i e_j}(\Omega) \langle e_j \rangle + \text{c.c.}$. Thus, when a depolarized field is subjected to direct photodetection, thermorefringent noise manifests as apparent intensity noise. That is one operational interpretation of the polarization noise plotted in Figs. 1 and 3.

Note that the photocurrent fluctuations emitted by the direct photodetection of a depolarized beam does not allow inference of the full polarization covariance matrix C_{ee} (and therefore its Fourier transform S_{ee}). In particular, for a choice of the input carrier polarization $\langle \mathbf{e} \rangle$, the photocurrent spectrum [Eq. (4.8)] is a linear combination of the elements of S_{ee} , from which the full matrix cannot be reconstructed. Indeed, attempts to assemble a set of measurements, by varying the mean input polarization, that is linearly independent in the elements of S_{ee} is not guaranteed to succeed in general, since changing the input polarization can change the transduction of the noise properties of the sample being interrogated (see Fig. 1, for example).

B. Balanced homodyne polarimetry

The most general type of optical detection that a polarized state of the optical field can be subjected to is balanced homodyne polarimetry. Here, the signal—the depolarized output of a system, represented by the electric field E_i in Eq. (4.1)—is mixed with a local oscillator (LO) in a pure and controllable polarization state that has a well-defined and controllable phase difference with the signal at a balanced polarizing beam-splitter; the resulting outputs are photodetected and their photocurrent subtracted. We will show that by controlling the local oscillator polarization and phase, the subtracted photocurrent can be used to deduce the spectral covariance matrix S_{ee} of the signal without changing the optical field used to probe the system.

We assume that the LO is prepared in the same transverse spatial mode f , and longitudinal mode with wave-vector k , as the signal of interest, so we take its electric field to be given by

$$E'_i = \langle E'_i \rangle = \sqrt{P'} e^{i(k_i z - \omega t)} f(x, y) \langle e'_i \rangle, \quad (4.9)$$

where $P' \gg P$ is the local oscillator power and e'_i its mean polarization. The assumption that the LO power is much larger than that of the signal effectively means that polarization fluctuations in the LO can be neglected, which is tacit in the above ansatz and in all that follows. This field is superposed with the signal at a balanced beam-splitter; the fields at its output are given by

$$E_i^\pm = \frac{1}{\sqrt{2}} (E'_i \pm E_i) \approx \frac{1}{\sqrt{2}} (\langle E'_i \rangle \pm \delta E_i), \quad (4.10)$$

where the second equality uses the fact that the LO is overwhelmingly more powerful than the signal (i.e., $P' \gg P$) and so neglects a term of order $\sqrt{P/P'}$. Each of the outputs is passed through a polarization analyzer (“polarizer”) which projects the polarization vector onto a chosen direction; this can be modelled by the transformation,

$$E_i^\pm \mapsto J_{ij}^\pm E_j^\pm, \quad (4.11)$$

where the projective nature of the polarizer implies that the Jones matrices \mathbf{J}^\pm satisfy $\mathbf{J}^\pm = (\mathbf{J}^\pm)^\dagger = (\mathbf{J}^\pm)^2$. These fields are individually detected, producing the photocurrents,

$$I^\pm = \alpha \int_{\mathcal{D}} d^2\mathbf{r} (J_{ij}^\pm E_j^\pm)^* (J_{ik}^\pm E_k^\pm), \quad (4.12)$$

where the integrands are evaluated at the detector plane $z = \ell$. Combining the above equations it can be shown that the fluctuations in these photocurrents are given by

$$\delta I^\pm = \pm \frac{\alpha}{2} \int_{\mathcal{D}} d^2\mathbf{r} [\langle E'_i \rangle^* J_{ij}^\pm \delta E_j + \text{c.c.}].$$

The individual photocurrents are subtracted to produce the homodyne photocurrent $I = I^+ - I^-$, whose fluctuations assume the form,

$$\delta I_{\text{hom}} = \frac{\alpha}{2} \int_{\mathcal{D}} d^2\mathbf{r} [\langle E'_i \rangle^* (J_{ij}^+ + J_{ij}^-) \delta E_j + \text{c.c.}]. \quad (4.13)$$

In order to maximize the sensitivity of the subtracted photocurrent to fluctuations in the signal field, it is best to choose polarizers that are orthogonal, in which case $\mathbf{J}^+ \mathbf{J}^- = \mathbf{0}$ and $\mathbf{J}^+ + \mathbf{J}^- = \mathbf{1}$. Physically, this choice corresponds to the intuition that each photodetector be sensitive to polarization fluctuations in orthogonal directions, so that their equal-weight superposition contains full information of both polarization components [84]. With this choice

$$\delta I_{\text{hom}} = \frac{\alpha}{2} \int_{\mathcal{D}} d^2\mathbf{r} [\langle E'_i \rangle^* \delta E_i + \text{c.c.}], \quad (4.14)$$

similar to the case of direct photodetection, except that the signal field fluctuations that are transduced are the ones that lie along the polarization of the mean LO field.

Inserting the explicit forms of the LO and signal fields [Eqs. (4.2) and (4.9)], the homodyne photocurrent fluctuations in Eq. (4.14) becomes,

$$\delta I_{\text{hom}} = \frac{\alpha}{2} \sqrt{PP'} [\langle e'_i \rangle^* J_{ij} \delta e_j + \text{c.c.}], \quad (4.15)$$

where ϕ is the common difference between the longitudinal modes of the LO and signal, and

$$\mathbf{J} = \begin{bmatrix} e^{ik(n_x-1)\ell} & 0 \\ 0 & e^{ik(n_y-1)\ell} \end{bmatrix}$$

is the Jones matrix describing the phase retardation between the LO and signal carrier polarizations as they propagate through to the photodetectors. Indeed by setting $\langle e''_j \rangle = J_{ji}^* \langle e'_i \rangle$, the photocurrent fluctuations can be seen to be proportional to $\langle e''_j \rangle^* \delta e_j + \text{c.c.}$, where $\langle e''_j \rangle$ can be identified with the polarization state of the LO after passing through a phase retarder described by the Jones matrix \mathbf{J}^\dagger . In this sense, if the LO polarization state is completely controllable, the effect of \mathbf{J} can in principle be absorbed into the definition of \mathbf{e}' ; we do so in the following. Computing the two-time correlation of the photocurrent fluctuations in Eq. (4.15), omitting terms that are non-stationary, and computing the Fourier transform, gives the photocurrent spectral density,

$$S_{II}^{\text{hom}}(\Omega) = \left(\frac{\alpha}{2} (PP')^{1/2} \right)^2 [\langle e'_i \rangle^* S_{e_i e_j}(\Omega) \langle e'_j \rangle + \text{c.c.}]. \quad (4.16)$$

In contrast with the case of direct photodetection [Eq. (4.8)], by changing the LO polarization \mathbf{e}' , all elements of the spectral covariance matrix of the signal polarization can be measured without perturbing the field incident on the sample.

Note that in general polarization fluctuations contaminate the homodyne photocurrent in all quadratures. To see this, re-introduce the phase retardation between the LO and signal, $\langle e'_i \rangle \rightarrow \langle e'_i \rangle e^{i\phi_i}$, and notice that whatever value of the relative phase ϕ_i is chosen, the photocurrent spectral density S_{II} is generically nonzero. In this sense, thermofringent noise can limit the sensitivity of an interferometric measurement in all quadratures. This is nothing but the manifestation of the fact that the noisy polarization state of the signal cannot perfectly interfere with the pure-polarized LO—a fact that is independent of signal quadrature.

C. Coherent cancellation of thermorefringent noise in signal detection

In the context of sensitive polarimetry experiments, the fact that thermorefringent noise is always lesser in the polarization state orthogonal to the probe field, i.e., $S_{e_y e_y} < S_{e_x e_x}$, suggests arranging the experiment so that the signal of interest is produced in that polarization, i.e., δe_y^{sig} . The resulting signal from a balanced homodyne polarimeter with LO state $\mathbf{e}' = (\cos \theta, e^{i\phi} \sin \theta)$ is

$$\begin{aligned} S_{II}^{\text{hom}} &\propto S_{e_y e_y}^{\text{sig}} + [S_{e_y e_y} + \cot^2(\theta) S_{e_x e_x} \\ &\quad + 2 \cot(\theta) \text{Re}\{e^{i\phi} S_{e_x e_y}^*\}] \\ &\equiv S_{e_y e_y}^{\text{sig}} + S_{e_y e_y}^{\text{app}}, \end{aligned} \quad (4.17)$$

which is Eq. (4.16) referred to the polarization signal of interest. The terms in the brackets in the first line represent the apparent signal arising from thermorefringent noise, denoted $S_{e_y e_y}^{\text{app}}$. The primary objective of any polarimetry experiment is the maximization of the signal-to-noise ratio $S_{e_y e_y}^{\text{sig}}/S_{e_y e_y}^{\text{app}}$; equivalently, the minimization of the noise $S_{e_y e_y}^{\text{app}}$ once the signal is fixed.

If there existed no correlations between thermorefringent noise of orthogonal polarizations (i.e., $S_{e_x e_y} = 0$), then, $S_{e_y e_y}^{\text{app}} = S_{e_y e_y} + \cot^2(\theta) S_{e_x e_x}$. This can be minimized by choosing LO tuned to the signal polarization, i.e., $\theta = \pi/2$, in which case the sensitivity to signal polarization is limited by thermorefringent noise in the same polarization (i.e., $S_{e_y e_y}$). Indeed this signal extraction strategy is conventionally practised for a different reason; to avoid extraneous background from the probe field.

However, since thermorefringent noise is correlated across the probe and signal polarizations (i.e., $S_{e_x e_y} \neq 0$, as seen in Fig. 1), better signal extraction strategies that harness these correlations can be imagined. Mathematically, the LO polarization angles (θ, ϕ) can be chosen so that the negative values of the correlation terms in $S_{e_y e_y}^{\text{app}}$ cancel with the positive terms. Expressing $S_{e_y e_y}^{\text{app}}$ by completing squares on $\cot \theta$, we find

$$\begin{aligned} S_{e_y e_y}^{\text{app}} &= S_{e_y e_y} - \frac{\text{Re}\{e^{i\phi} S_{e_x e_y}^*\}^2}{S_{e_x e_x}} \\ &\quad + [\cot \theta \cdot S_{e_x e_x} + \text{Re}\{e^{i\phi} S_{e_x e_y}^*\}]^2. \end{aligned} \quad (4.18)$$

It is clear that this is minimized at a Fourier frequency of interest Ω when the second term is maximized by proper choice of ϕ , and the third term is nulled by choice of θ . Noting that $\text{Re}\{e^{i\phi} S_{e_x e_y}^*\}^2 = |S_{e_x e_y}^2| \cos^2(\phi - \arg S_{e_x e_y})$, these optimal choices are

$$\begin{aligned} \phi_{\text{opt}}(\Omega) &= \arg S_{e_x e_y}[\Omega] \\ \theta_{\text{opt}}(\Omega) &= \cot^{-1} \frac{-\text{Re}\{e^{i\phi} S_{e_x e_y}^*[\Omega]\}}{S_{e_x e_x}[\Omega]}. \end{aligned} \quad (4.19)$$

With this choice, the noise at that frequency is

$$S_{e_y e_y}^{\text{app}}(\Omega)|_{\theta_{\text{opt}}, \phi_{\text{opt}}} = S_{e_y e_y}(\Omega) \left[1 - \frac{|S_{e_x e_y}^2(\Omega)|}{S_{e_x e_x}(\Omega) S_{e_y e_y}(\Omega)} \right]. \quad (4.20)$$

Since the correlation is bounded by the Cauchy-Schwarz inequality $|S_{e_x e_y}^2| \leq S_{e_x e_x} S_{e_y e_y}$, in principle, perfect cancellation at a desired Fourier frequency is possible if the correlations are perfect (i.e., saturate the inequality). Even with imperfect correlations, narrow-band evasion of thermorefringent noise is possible via balanced homodyne polarimetry via coherent cancellation. This strategy always outperforms—in a narrow-band of choice—the conventional signal extraction strategy of tuning the LO to a polarization orthogonal to the probe.

V. CONCLUSIONS

Having emerged from the thicket, we can now contextualize thermorefringent noise in the wider landscape of thermo-optic noises. Fluctuations of the apparent temperature of amorphous materials cause their optical properties to fluctuate, which can manifest as extraneous noise in precision optical measurements [1]. The most insidious source of such thermo-optic noise is that due to fluctuations in the thickness of coatings on mirrors, the intensity of which is related to the mechanical loss of these materials. Driven by the idea that it is the glassy energy landscape of amorphous materials that gives rise to mechanical dissipation [85–88], a concerted effort to discover more pristine materials has ensued in communities engaged in precision optical measurements. Recent measurements [28,29] have unearthed evidence that crystalline materials may offer some refuge from thermo-optic noises because of the absence of glassy behavior. In the current study, we have demonstrated that precisely because of the anisotropy of the crystalline state, qualitatively novel sources of thermodynamically driven optical noises can arise.

In particular, fluctuations in temperature can be anisotropic, which drive fluctuations in the dielectric tensor of the medium, resulting in the polarization of an incident optical field to transmute into an impure state. We term this thermorefringent noise. An impure polarization state manifests in optical measurements via its inability to interfere perfectly with a reference pure-polarized field. The result is that thermorefringent noise can manifest as apparent noise in any quadrature of the optical field, quite unlike thermo-optic noise from amorphous media. There are also other manifestations of thermorefringent noise, such as the thermal scattering of light into orthogonal polarizations,

which can be detrimental to precision polarimetry experiments. In addition, we also discover that thermodynamic scattering into higher-order spatial modes is possible, even in amorphous optical media.

The phenomenology of thermorefringent noise critically depends on the temperature-dependent parts of the dielectric tensor, which can in turn depend on residual stresses on optical materials such as coatings. These poorly understood aspects of such materials need to be carefully characterized to ascertain the realistic limits that thermorefringent noise will place on precision optical measurements.

We have also proposed a novel signal extraction strategy employing balanced homodyne polarimetry which can coherently cancel thermorefringent noise. This technique crucially relies on the complete theoretical understanding of thermo-optic noises that our formalism has captured, including thermodynamically induced correlations in the optical polarization. The coherent cancellation strategy can evade correlated polarization noise in a narrow frequency of choice by simple tuning of the local oscillator polarization state, and is only limited by the strength of the correlations.

ACKNOWLEDGMENTS

We thank Sergey Vyatchanin for a discussion about the fluctuation-dissipation theorem for the heat equation, and Matt Evans for motivating us to reconcile our approach with that via Levin’s “direct approach” (the result is Appendix D 5). S. K. and V. S. were partly supported by the Reed Award of the MIT School of Engineering. E. D. H. is supported by the MathWorks, Inc. This work has Document No. LIGO–P2100419.

APPENDIX A: DIRECTIONAL CORRELATION OF THERMAL NOISE

In this appendix we consider the general problem of reconciling the microscopic anisotropic description of the temperature field u , given in Eqs. (2.3) and (2.4), with the macroscopic thermodynamic expectation for the temperature, given in Eq. (2.1).

If we assume that the noise $\zeta_i(\mathbf{r}, t)$ is uncorrelated across space and time, the only remaining source of correlation are directional. Since there are only three second rank tensors dictated by the system, namely δ_{ij} , D_{ij} , $(D^{-1})_{ij}$, any directional correlation must be captured in the general expression

$$\langle \zeta_i(\mathbf{r}, t) \zeta_j(\mathbf{r}', t') \rangle = (\zeta_0^2 \delta_{ij} + \zeta_1^2 D_{ij} + \zeta_{-1}^2 D_{ij}^{-1}) \times \delta(\mathbf{r} - \mathbf{r}') \delta(t - t'), \quad (\text{A1})$$

where $\zeta_{-1,0,1}$ are scalars to be determined.

According to Eq. (2.6) the local temperature u is driven by the noise $\eta = \partial_i \zeta_i$. The above choice for ζ_i implies that the Fourier transform, $\eta(\mathbf{K}, \Omega) = \int d\mathbf{r} dt \eta(\mathbf{r}, t) e^{-i(\mathbf{K}\cdot\mathbf{r} - \Omega t)}$, is characterized by

$$\begin{aligned} & \langle \eta(\mathbf{K}, \Omega) \eta^*(\mathbf{K}', \Omega') \rangle \\ &= (\zeta_0^2 K_i K_j + \zeta_1^2 D_{ij} K_i K_j + \zeta_{-1}^2 D_{ij}^{-1} K_i K_j) \\ & \times (2\pi)^4 \delta(\mathbf{K} - \mathbf{K}') \delta(\Omega - \Omega'). \end{aligned} \quad (\text{A2})$$

Since the relation between the local temperature u and η is linear [Eq. (2.6)], it can be solved via a Fourier transform to produce

$$\langle u(\mathbf{K}, \Omega) u^*(\mathbf{K}', \Omega') \rangle = \frac{\langle \eta(\mathbf{K}, \Omega) \eta^*(\mathbf{K}', \Omega') \rangle}{(-i\Omega + D_{ij} K_i K_j)(i\Omega' + D_{ij} K'_i K'_j)}. \quad (\text{A3})$$

The scalars $\zeta_{-1,0,1}$ that determine the nature of the directional correlation of the noise ζ_i [Eq. (A1)] need to be such that the thermodynamic relation for the macroscopic temperature [Eq. (2.1)], $\text{Var}[T] = k_B T^2 / C_V$ is consistent with the volume-average of the microscopic temperature u . That is, we demand,

$$\begin{aligned} \frac{k_B T^2}{C_V} &= \text{Var}[T] \\ &= \frac{1}{V} \int_V dV \frac{1}{V'} \int_{V'} dV' \langle u(\mathbf{r}, t) u^*(\mathbf{r}', t) \rangle, \end{aligned} \quad (\text{A4})$$

where

$$\begin{aligned} \langle u(\mathbf{r}, t) u(\mathbf{r}', t) \rangle &= \int \frac{d\mathbf{K} d\Omega d\mathbf{K}' d\Omega'}{(2\pi)^8} \\ & \times \langle u(\mathbf{K}, \Omega) u^*(\mathbf{K}', \Omega') \rangle e^{i(\Omega - \Omega')t} e^{i(\mathbf{K}\cdot\mathbf{r} - \mathbf{K}'\cdot\mathbf{r}')}, \end{aligned} \quad (\text{A5})$$

The integral in equation Eq. (A5) can be reduced to,

$$\begin{aligned} \langle u(\mathbf{r}, t) u(\mathbf{r}', t) \rangle &= \int \frac{d\mathbf{K}}{(2\pi)^3} \frac{e^{i\mathbf{K}\cdot(\mathbf{r} - \mathbf{r}')}}{2} \\ & \times \frac{(\zeta_0^2 K_i K_i + \zeta_1^2 D_{ij} K_i K_j + \zeta_{-1}^2 D_{ij}^{-1} K_j K_i)}{D_{ij} K_i K_j}. \end{aligned} \quad (\text{A6})$$

The fraction in the second line of the integrand has an essential discontinuity at $\mathbf{K} = 0$, unless $\zeta_0 = \zeta_{-1} = 0$ or D_{ij} is proportional to identity matrix.

The discontinuity dictates the value of the integral, and we will show that the integral is multivalued, unless there is no discontinuity. In case of isotropic medium, the integral in Eq. (A6) returns a value proportional to $\delta(\mathbf{r} - \mathbf{r}')$ (see Appendix B in [26]). In that case, asymptotics of the integrand at $\mathbf{K} = 0$ defines the proportionality coefficient ζ_1^2 . In the case of anisotropic medium, the scalars $\zeta_{0,1}$ can in principle contribute. To study their contributions, we will perform the integral. First, we separate the integral into three terms,

$$\langle u(\mathbf{r}, t)u(\mathbf{r}', t) \rangle_\alpha = \int \frac{d\mathbf{K}}{(2\pi)^3} \frac{F_\alpha(\mathbf{K})}{2} e^{i\mathbf{K}\mathbf{r} - i\mathbf{K}'\mathbf{r}'}, \quad (\text{A7})$$

where, $F_0(\mathbf{K}) = \zeta_0^2 K_i K_i / D_{ij} K_i K_j$, the second integrand $F_1(\mathbf{K}) = \zeta_1^2 D_{ij} K_i K_i / D_{ij} K_i K_j = \zeta_1^2$, and the third, $F_{-1}(\mathbf{K}) = \zeta_{-1}^2 D_{ij}^{-1} K_i K_i / D_{ij} K_i K_j$. Then the correlation in the physical temperature fluctuations can be expressed as the sum,

$$\langle u(\mathbf{r}, t)u(\mathbf{r}', t) \rangle = \sum_{\alpha \in \{0, \pm 1\}} \langle u(\mathbf{r}, t)u(\mathbf{r}', t) \rangle_\alpha. \quad (\text{A8})$$

We now compute each of the terms in the sum.

The integral for $F_1(\mathbf{K})$ is reduced to a δ -function, since $F_1(\mathbf{K})$ doesn't have an essential discontinuity at $\mathbf{K} = 0$:

$$\langle u(\mathbf{r}, t)u(\mathbf{r}', t) \rangle_0 = \frac{\zeta_0^2}{2} \int \frac{\tilde{K}^2 \sin \theta d\tilde{K} d\theta}{(2\pi)^2 \sqrt{\det \mathbf{D}}} e^{i\tilde{\mathbf{K}}v \cos \theta} \times \left[\frac{1}{2} \left(\frac{1}{D_x} + \frac{1}{D_y} \right) \sin^2 \theta + \frac{1}{D_z} \cos^2 \theta \right].$$

Performing the polar integral gives

$$\langle u(\mathbf{r}, t)u(\mathbf{r}', t) \rangle_0 = \frac{\zeta_0^2}{2} \left\{ (4D_z^{-1} - \text{Tr}(\mathbf{D}^{-1}))\delta(\mathbf{r} - \mathbf{r}') - \frac{3D_z^{-1} - \text{Tr}(\mathbf{D}^{-1})}{4\pi\sqrt{\det \mathbf{D}}} \times \frac{1}{(D_{ij}^{-1}(r_i - r'_i)(r_j - r'_j))^{3/2}} \right\}. \quad (\text{A10})$$

The integral containing $F_{-1}(\mathbf{K})$ can be computed applying the same method,

$$\langle u(\mathbf{r}, t)u(\mathbf{r}', t) \rangle_{-1} = \frac{\zeta_{-1}^2}{2} \left\{ (4D_z^{-2} - \text{Tr}(\mathbf{D}^{-2}))\delta(\mathbf{r} - \mathbf{r}') - \frac{3D_z^{-2} - \text{Tr}(\mathbf{D}^{-2})}{4\pi\sqrt{\det \mathbf{D}}} \times \frac{1}{(D_{ij}^{-1}(r_i - r'_i)(r_j - r'_j))^{3/2}} \right\}. \quad (\text{A11})$$

Note however that the expressions in Eqs. (A10) and (A11) are unphysical in a subtle manner. In fact the essential discontinuity in the integrands in Eq. (A6) that are proportional to renders their integral multivalued. This can be seen from the result in Eqs. (A10) and (A11) where the z direction take a privileged position despite no such asymmetry in the integrand. This origin of this asymmetry is the order in which the integral is performed in the generalized spherical coordinates. The multivalued integral in this case is unphysical and, as expected, puts constraints on the form of the correlation of the noise term ζ .

One case, when the integral is single-valued corresponds to $\zeta_0 = \zeta_{-1} = 0$. In this case the singularity at coordinate origin is absent, and the noise is completely described by one term,

$$\langle \zeta_i(\mathbf{r}, t)\zeta_j(\mathbf{r}', t) \rangle = \zeta_1^2 D_{ij} \delta(\mathbf{r} - \mathbf{r}') \delta(t - t'). \quad (\text{A12})$$

The second case is less trivial and involves exploring the structure of Eqs. (A10) and (A11). The integrals in these equations could be computed the same way, but with

$$\langle u(\mathbf{r}, t)u(\mathbf{r}', t) \rangle_1 = \frac{\zeta_1^2}{2} \delta(\mathbf{r} - \mathbf{r}'). \quad (\text{A9})$$

The integrals containing $F_{0,1}(\mathbf{K})$ are more complicated, but both of them are computable in the same fashion, namely by changing variables to generalized spherical coordinates. For easier pedagogy we perform the variable substitution in steps. As a first step, we consider the basis in which D_{ij} is diagonalized (it can be, since it is symmetric) with eigenvalues D_i . We perform a substitution $\tilde{K}_i = \sqrt{D_i} K_i$, $v_i = (r_i - r'_i) / \sqrt{D_i}$ to get rid of D_{ij} in the denominator. Then we rotate the resulting coordinate system so as to make \mathbf{v} lie along the z -direction of the rotated system. Finally, the $\tilde{\mathbf{K}}$ integration is performed in spherical coordinates. The integral containing F_0 then takes the form

different axis choice for the spherical coordinates. If the axis is chosen along D_x or D_y (instead of D_z as above), the D_i -dependent pre-factors on the right hand sides of Eqs. (A10) and (A11) would take a different form. The necessary condition for the integral to be single-valued is the equality among these prefactors (independent of the choice of integration variables). For example, if one considers the coefficient for the second term in the Eq. (A10), one obtains the system of equations:

$$\begin{aligned} 2D_z^{-1} - D_x^{-1} - D_y^{-1} &= 2D_x^{-1} - D_y^{-1} - D_z^{-1}, \\ 2D_z^{-1} - D_x^{-1} - D_y^{-1} &= 2D_y^{-1} - D_x^{-1} - D_z^{-1}, \end{aligned}$$

whose only solution is $D_x = D_y = D_z$. When this condition is satisfied the essential discontinuity in the original integral also vanishes, rendering the integral single valued. Physically this case corresponds to that of a material with isotropic thermal diffusion. Mathematically, this is already included in the case corresponding to $\zeta_0 = \zeta_{-1} = 0$. Thus, the latter is the only case to be considered.

Finally, ζ_1 can be computed using Eq. (A4),

$$\frac{k_B T^2}{C_V} = \frac{\zeta_1^2}{2V} \quad (\text{A13})$$

Our result reproduces the typical results for the isotropic medium, for example [26].

APPENDIX B: ORIGIN OF ϵ'_{xy} AND MATERIAL PARAMETERS

In this appendix we concern ourselves with how a nonzero ϵ'_{xy} can arise. One possibility is through photoelasticity, in which applied stress produces changes in the permittivity tensor. An applied stress σ_{ij} is linearly related to changes in the inverse dielectric tensor $B_{ij} = (\epsilon^{-1})_{ij}$ by $\delta B_{ij} = \pi_{ijkl} \sigma_{kl}$. To first order, perturbations in B_{ij} are related to perturbations in ϵ_{ij} by $\delta \epsilon_{il} = -\epsilon_{ij} \delta B_{jk} \epsilon_{kl}$. In particular, even in a system in which the unperturbed ϵ_{ij} is diagonal, an off-diagonal perturbation can appear as $\delta \epsilon_{xy} = -\epsilon_{xx} \delta B_{xy} \epsilon_{yy}$. The way in which stresses can produce a nonzero δB_{xy} depends on the particular crystal structure; even in cubic crystals (and isotropic materials), a shear strain σ_{xy} will produce a nonzero δB_{xy} via a nonzero π_{xyxy} (in Voigt notation, π_{66} , which for cubic and isotropic materials is identical to π_{44}) [78]. A temperature-dependent term ϵ'_{xy} can then arise either via a temperature dependence of π_{xyxy} or of σ_{xy} [89].

APPENDIX C: FIELD EVOLUTION WITH SMALL PERTURBATIONS

In this appendix we provide some details of the passage from the equations for the electromagnetic field [Eq. (2.13)] to equations for the polarization fluctuations [Eq. (3.1)].

To derive the necessary equations we will apply several assumptions about the configuration of electromagnetic field [notation from Eqs. (2.12) and (2.13)],

- (i) We assume that the transverse spatial mode f_0 of the incident field is gaussian and that its width is much greater than the wavelength and temperature fluctuations scale (this is typically true for macroscopic mirrors, as estimated in Ref. [4]). This provides us several estimates for derivatives of the main mode: $|\nabla f_0| \ll |k f_0|$, $|\nabla \delta e_i^{(0)}| \ll |k \delta e_i^{(0)}|$, $|\delta e_i^{(0)} \nabla f_0| \ll |f_0 \nabla \delta e_i^{(0)}|$.
- (ii) We assume that noise source frequency scale is much lower than the optical frequency. This gives us estimates of time derivatives of the fluctuations in the electromagnetic field, $|\partial_t \delta e_i^{(\alpha)}| \ll |\omega \delta e_i^{(\alpha)}|$.

We plug the expansion Eq. (2.13) into Eq. (2.11) and project it onto the basis function f_α . The projection of various terms in the equation are as follows:

$$(f_\alpha | \partial_t^2 \langle E_x \rangle) = \sqrt{P} e^{i(kn_x z - \omega t)} (-\omega^2 \delta_{0\alpha}) \langle e_x^{(0)} \rangle \quad (\text{C1})$$

$$(f_\alpha | \partial_t^2 \delta E_x) = \sqrt{P} e^{i(kn_x z - \omega t)} \times (-\omega^2 \delta e_x^{(\alpha)} - 2i\omega \partial_t \delta e_x^{(\alpha)} + \partial_t^2 \delta e_x^{(\alpha)}). \quad (\text{C2})$$

In the formula below we use notation $\Delta_{xy} = \partial_x^2 + \partial_y^2$:

$$(f_\alpha | \Delta_{xy} \delta E_x) = \sqrt{P} e^{i(kn_x z - \omega t)} \left[\sum_\beta (f_\alpha | \Delta_{xy} f_\beta) \delta e_x^{(\beta)} - k^2 n_x^2 \delta e_x^{(\alpha)} + 2ikn_x \left(\frac{\partial}{\partial z} \delta e_x^{(\alpha)} \right) + \frac{\partial^2}{\partial z^2} \delta e_x^{(\alpha)} \right] \quad (\text{C3})$$

TABLE I. Parameters for crystalline materials. Values for silicon were taken from Refs. [66–69]; values for lithium niobate were taken from Refs. [70–72]; values for GaAs/AlGaAs were taken from Refs. [73–75]. The heat capacity values here suffice for both constant-volume and constant-pressure situations, since these solids are only weakly compressible. The aluminum alloying fraction for AlGaAs was assumed to be 92%. An asterisk indicates that the value was chosen *ad hoc*. A dagger indicates that the tensor values have been assumed from scalar measurements.

Quantity	Symbol	Si	LiNbO ₃	GaAs	AlGaAs	Unit
Temperature	T	123	293	293	293	K
Density	ρ	2330	4630	5320	3860	kg m ⁻³
Heat capacity per unit mass	C	330	640	320	440	J kg ⁻¹ K ⁻¹
Thermal conductivity	$\left\{ \begin{array}{l} \kappa_{xx} \\ \kappa_{yy} \\ \kappa_{zz} \end{array} \right.$	600 [†]	4.5	44 [†]	71 [†]	W m ⁻¹ K ⁻¹
		600 [†]	4.4	44 [†]	71 [†]	W m ⁻¹ K ⁻¹
		600 [†]	4.5	44 [†]	71 [†]	W m ⁻¹ K ⁻¹
Laser wavelength in vacuum	λ	1550	1550	1550	1550	nm
Refractive indices	$\left\{ \begin{array}{l} n_x \\ n_y \end{array} \right.$	3.46	2.14	3.37	2.90	...
		3.46	2.21	3.37	2.90	...
Thermorefractive coefficients	$\left\{ \begin{array}{l} \epsilon'_{xx} \\ \epsilon'_{yy} \\ \epsilon'_{xy} \end{array} \right.$	700	130	1370	1020	ppm K ⁻¹
		700	-1	1370	1020	ppm K ⁻¹
		10*	1*	10*	10*	ppm K ⁻¹

$$\begin{aligned}
(f_\alpha|\partial_x\nabla\cdot\delta\mathbf{E}) &= \sqrt{P}\sum_\beta\left[e^{i(kn_xz-\omega t)}(f_\alpha|\partial_x^2f_\beta)\delta e_x^{(\beta)}\right. \\
&\quad + e^{i(kn_yz-\omega t)}(f_\alpha|\partial_x\partial_yf_\beta)\delta e_y^{(\beta)} \\
&\quad \left.+ e^{i(kn_zz-\omega t)}(f_\alpha|\partial_xf_\beta)\frac{\partial}{\partial z}\delta e_z^{(\beta)}\right] \quad (\text{C4})
\end{aligned}$$

The most important case is $\alpha = 0$, since this is the projection with the highest overlap with noise source. Several terms in the above sums can be neglected as follows:

- (i) The condition $|\partial_t\delta e_i^{(0)}| \ll |\omega\delta e_i^{(0)}|$ allows us to neglect $\partial_t^2\delta e_x^{(0)}$ term in Eq. (C2).
- (ii) The relation $(f_\alpha|\partial_xf_\beta) = -(f_\beta|\partial_xf_\alpha)$ show that all terms of the form $(f_\alpha|\partial_xf_\beta)$ are of the order of magnitude $1/r_0$ (r_0 is a laser beam radius), when $\alpha \sim 1$. Using the estimate, $|\nabla f_0| \ll |kf_0|$, terms like, $(f_\alpha|\Delta_{xy}|f_\beta)$ and $\partial_z^2\delta e_x^{(\alpha)}$ in Eqs. (C3) and (C4) can be neglected for $\alpha = 0$.

Thus simplified, Eqs. (C1)–(C4) can be substituted into Eq. (2.11), and the $\alpha = 0$ term isolated. This gives the system of equations in Eq. (3.1).

APPENDIX D: LIMITING FORMS OF POLARIZATION SPECTRAL DENSITIES IN TRANSMISSION

The expression for the polarization spectral densities for transmission through a crystalline material—given in Eqs. (3.10)–(3.12)—can be reduced in various limiting cases to much simpler forms. We exhibit some of these limiting cases in this appendix. Finally, in Appendix D 4, we provide an alternate calculation of $S_{e_x e_x}$ in the fully adiabatic regime, as an independent check of the full theory in Sec. III B of the main text.

1. Asymptotic expansion of thermal integral

The thermal integral [Eq. (3.13)],

$$I(\Omega_1, \Omega_2) = \int_0^\infty d\tau \frac{\cos \Omega_1 \tau \exp(-\Omega_2^2 D_{zz} \tau / c^2)}{\sqrt{(\tau + \tau_x)(\tau + \tau_y)}},$$

dictates the frequency dependence of the polarization fluctuations for transmission through a crystalline medium. In order to deduce limiting forms of the polarization fluctuations in the various frequency regimes of interest, it is germane to study the asymptotic properties of this integral. That integral can be written as

$$\begin{aligned}
I(\Omega_1, \Omega_2) &= \sum_{n=0}^{+\infty} C_n \left(\frac{\tau_-}{\tau_+}\right)^{2n} \text{Re} \left[e^{-i\Omega_1 \tau_+} \exp\left(\frac{\Omega_2^2}{c^2} D_{zz} \tau_+\right) \right. \\
&\quad \left. \times \text{Ei}_{2n+1}\left(-i\Omega_1 \tau_+ + \frac{\Omega_2^2}{c^2} D_{zz} \tau_+\right) \right], \quad (\text{D1})
\end{aligned}$$

where $\tau_\pm = |\tau_x \pm \tau_y|/2$, C_n are the coefficients in the Taylor series expansion of function $1/\sqrt{1-x}$ around $x = 0$, and Ei_n stand for the n^{th} order exponential integral defined by, $\text{Ei}_m(z) = \int_1^\infty dt t^{-m} e^{-zt}$, for $\text{Re}\{z\} \geq 0$ and $m > 0$. (Note that the above expansion for the integral I reduces to the result obtained previously for the special case of an isotropic medium [90]—i.e., all terms vanish except for $n = 0$.) The physically interesting cases correspond to the argument of Ei_n approaching zero or infinity. The required asymptotic expansions are known for Ei_1 [[91], Sec. 2.3],

$$\text{Ei}_1(z) \approx \begin{cases} -\ln z - \gamma - \sum_{k=1}^{\infty} \frac{(-1)^k}{k!} \frac{z^k}{k}; & z \rightarrow 0 \\ \frac{e^{-z}}{z} \sum_{k=0}^N \frac{(-1)^k k!}{z^k} + O(|z|^{-N}); & z \rightarrow \infty \end{cases} \quad (\text{D2})$$

where $\gamma \approx 0.57721$ is Euler's constant, and these are valid respectively for $\arg z \neq \pi$, and $\arg z < \pi/2$. Expansions for $\text{Ei}_{n>1}$ can be computed from these via the recursion relation [91], $\text{Ei}_{n+1}(z) = \int_z^\infty dz' \text{Ei}_n(z')$. This relation implies that $\text{Ei}_n(z) = o(\text{Ei}_1(z))$ for $n > 1$ when $z \rightarrow 0$, and $\text{Ei}_n(z) \sim \text{Ei}_1(z)$ when $z \rightarrow +\infty$ [92]. Therefore, only the first term in the series expansion for I in Eq. (D1) contributes for small arguments, and all the terms contribute the same amount for large arguments. Therefore both of the cases are solely described by the corresponding asymptotic expression for Ei_1 .

The above asymptotic expansions, handled carefully respecting the domain of the complex argument of Ei_n in Eq. (D1), produces the following limiting cases.

2. Limiting forms of $S_{e_x e_x}$

There are two physically interesting regimes for $S_{e_x e_x}$. The first regime is the small-frequency limit, $n_x^2 D_{zz} \tau_+ \Omega^2 / c^2 \ll \Omega \tau_+ \ll 1$. In this regime the power spectral density shows logarithmic behavior,

$$S_{e_x e_x}(\Omega) = -\frac{k^2 \xi^2 |\epsilon'_{xx}|^2 \ell}{16\pi n_x^2 \sqrt{D_{yy} D_{xx}}} \ln(|\Omega \tau_+|) \quad (\text{D3})$$

The second physically interesting regime typically corresponds to the situation when Ω is big enough that $1 \ll \Omega \tau_+$, but still small enough for the noise to be quasistatic, i.e., $n_x^2 D_{zz} \tau_+ \Omega^2 / c^2 \ll \Omega \tau_+$. This results in the following behavior. In this regime the power spectral density shows inverse square behavior,

$$S_{e_x e_x}(\Omega) = \frac{k^2 \xi^2 |\epsilon'_{xx}|^2 \ell \tau_+}{8\pi n_x^2 r_0^2} \frac{1}{|\Omega \tau_+|^2}. \quad (\text{D4})$$

3. Limiting forms of $S_{e_y e_y}$ and $S_{e_x e_y}$

In addition to other parameters, power spectral densities $S_{e_x e_y}$ and $S_{e_y e_y}$ acquire additional frequencylike parameter $\omega \Delta n$, where $\Delta n = n_x - n_y$. This results in three physically interesting regimes. The first one corresponds to the small

Ω limit when $\Omega\tau_+ \ll D_{zz}\tau_+\omega^2(\Delta n)^2/c^2 \ll 1$. In this regime the power spectral density is frequency independent,

$$S_{e_y e_y}(\Omega) = -\frac{k^2 \zeta^2 |\epsilon'_{xy}|^2 \ell}{16\pi n_y^2 \sqrt{D_{yy} D_{xx}}} \ln \left[\left| D_{zz} \tau_+ (\Delta n)^2 \frac{\omega^2}{c^2} \right| \right], \quad (\text{D5})$$

$$S_{e_x e_y}(\Omega) = \frac{k^2 \zeta^2 \epsilon'_{xy} \epsilon'_{xx} \ell}{16\pi n_x n_y \sqrt{D_{yy} D_{xx}}} \ln \left[\left| D_{zz} \tau_+ (\Delta n)^2 \frac{\omega^2}{c^2} \right| \right] \times \frac{1 - \exp[-i\omega\ell \Delta n/c]}{\omega\ell \Delta n/c}. \quad (\text{D6})$$

The next regime corresponds to the transient Ω when $D_{zz}\tau_+\omega^2(\Delta n)^2/c^2 \ll \Omega\tau_+ \ll 1$. In this regime the power spectral density shows logarithmic behavior,

$$S_{e_y e_y}(\Omega) = -\frac{k^2 \zeta^2 |\epsilon'_{xy}|^2 \ell}{16\pi n_y^2 \sqrt{D_{yy} D_{xx}}} \ln(|\Omega\tau_+|), \quad (\text{D7})$$

$$S_{e_x e_y}(\Omega) = \frac{k^2 \zeta^2 \epsilon'_{xy} \epsilon'_{xx} \ell}{16\pi n_x n_y \sqrt{D_{yy} D_{xx}}} \ln(|\Omega\tau_+|) \times \frac{1 - \exp[-i\omega\ell \Delta n/c]}{\omega\ell \Delta n/c}. \quad (\text{D8})$$

Finally, there is the large Ω limit when $D_{zz}\tau_+\omega^2(\Delta n)^2/c^2 \ll \Omega\tau_+$ and $1 \ll \Omega\tau_+$. In this regime the power spectral density shows inverse square behavior

$$S_{e_y e_y}(\Omega) = \frac{k^2 \zeta^2 |\epsilon'_{xy}|^2 \ell \tau_+}{8\pi n_y^2 r_0^2} \frac{1}{|\Omega\tau_+|^2}, \quad (\text{D9})$$

$$S_{e_x e_y}(\Omega) = -\frac{k^2 \zeta^2 \epsilon'_{xy} \epsilon'_{xx} \ell \tau_+}{8\pi n_x n_y r_0^2} \frac{1}{|\Omega\tau_+|^2} \times \frac{1 - \exp[-i\omega\ell \Delta n/c]}{\omega\ell \Delta n/c}. \quad (\text{D10})$$

4. Adiabatic limit: Modal method

In many situations of interest, the characteristic size of the crystal is such that the temperature field is effectively static compared to the travel time of the light through the crystal ($\Omega\ell \ll c$), and the fluctuations are slow compared to the cycle of the carrier ($\Omega \ll \omega$). This ‘‘adiabatic’’ regime is the one considered by Braginsky and Vyatchanin [90] for the case of an amorphous material.

Here we generalize their method to the anisotropic case, with the aim of reproducing the predictions of our detailed model through an alternate route. The general strategy is to first compute the fluctuation in average temperature of the crystal volume probed by the laser beam, and then to propagate this to fluctuation in the polarization state of the light.

To find the average temperature, we start with the heat equation [Eq. (2.6)],

$$(\partial_t - D_{ij} \partial_i \partial_j) u(\mathbf{r}, t) = \eta(\mathbf{r}, t), \quad (\text{D11})$$

where η is a random heat injection with the correlation [Eq. (3.6)]

$$\langle \eta(\mathbf{r}, t) \eta(\mathbf{r}', t') \rangle = \zeta^2 D_{ij} \partial_i \partial_j \delta(\mathbf{r} - \mathbf{r}') \delta(t - t') \quad (\text{D12})$$

with $\zeta^2 = 2k_B T^2 / c_V$.

Given the boundary condition $\partial_z u = 0$ at $z = 0$ and $z = \ell$, we can write down a series solution

$$u(\mathbf{r}, t) = \int_{-\infty}^{\infty} \frac{dk_x dk_y d\Omega}{(2\pi)^3} \sum_n u_n(k_x, k_y, \Omega) e^{i\Omega t - ik_x x - ik_y y} \cos(b_n z) \quad (\text{D13})$$

with $b_n = \pi n / \ell$. Each coefficient,

$$u_n(k_x, k_y, \Omega) = \int_{-\infty}^{\infty} dx dy dt e^{-i\Omega t + ik_x x + ik_y y} \times \int_0^\ell dz \frac{2 - \delta_{0n}}{\ell} \cos(b_n z) u(x, y, z, t), \quad (\text{D14})$$

defines a mode of the local temperature field. Inserting the above expansion [Eq. (D13)] in the heat equation [Eq. (D11)], it is found that each mode is independent, and given by

$$u_n(k_x, k_y, \Omega) = \frac{\eta_n(k_x, k_y, \Omega)}{i\Omega - D_{ij} k_i k_j}, \quad (\text{D15})$$

where

$$\langle \eta_m(k_x, k_y, \Omega) \eta_n^*(k'_x, k'_y, \Omega') \rangle = (2\pi)^3 \zeta^2 D_{ij} k_i k_j \frac{2 - \delta_{0n}}{\ell} \delta_{mn} \delta(k_x - k'_x) \delta(k_y - k'_y) \delta(\Omega - \Omega'). \quad (\text{D16})$$

We now construct an *ad hoc* observable [61,62], the volume-averaged temperature over the cylindrical region of the beam (radius r_0) in the crystal (length ℓ),

$$\bar{u}(t) = \frac{1}{\pi r_0^2 \ell} \int_V d^3 \mathbf{r} e^{-(x^2+y^2)/r_0^2} u(\mathbf{r}, t) = \int_{-\infty}^{+\infty} \frac{dk_x dk_y d\Omega}{(2\pi)^3} e^{-r_0^2(k_x^2+k_y^2)/4} e^{i\Omega t} u_0(k_x, k_y, \Omega); \quad (\text{D17})$$

where we have dropped all terms in the Fourier series except for the $n = 0$ term, since this is the only term which has a nonzero integral in the z direction. We can compute the correlation function of this volume-averaged temperature, giving

$$\langle \bar{u}(t) \bar{u}(t + \tau) \rangle = \zeta^2 \times \frac{1}{\ell} \int_{-\infty}^{+\infty} \frac{dk_x dk_y d\Omega}{(2\pi)^3} e^{-r_0^2(k_x^2+k_y^2)/2} \frac{\mathfrak{D}(k_x, k_y) e^{i\Omega \tau}}{\Omega^2 + \mathfrak{D}(k_x, k_y)^2}, \quad (\text{D18})$$

where $\mathfrak{D}(k_x, k_y) = D_{xx}k_x^2 + 2D_{xy}k_xk_y + D_{yy}k_y^2$. Then since the correlation function is related to the two-sided spectral density $\mathcal{S}(\Omega)$ by $\langle \bar{u}(t) \bar{u}(t + \tau) \rangle = \frac{1}{2\pi} \int_{-\infty}^{+\infty} d\Omega \mathcal{S}(\Omega) e^{i\Omega \tau}$, we can immediately read off the one-sided spectral density $S(|\Omega|) = 2\mathcal{S}(\Omega)$ for the volume-averaged temperature,

$$S_{\bar{u}\bar{u}}(\Omega) = \frac{4k_B T^2}{c_V \ell} \int_{-\infty}^{+\infty} \frac{dk_x dk_y}{(2\pi)^2} \frac{\mathfrak{D}(k_x, k_y) e^{-r_0^2(k_x^2+k_y^2)/2}}{\Omega^2 + \mathfrak{D}(k_x, k_y)^2}, \quad (\text{D19})$$

which reduces to Eq. (E6) of Braginsky and Vyatchanin [90] in the thermally isotropic limit. Note that we did not use any assumption about the length scale of the crystal relative to the thermal diffusion wavelength in this derivation.

To complete the calculation, we need to connect fluctuations in $\bar{u}(t)$ to fluctuations in the optical field. The variable $\bar{u}(t)$ has been constructed so that in an optically isotropic material, the phase fluctuation of a passing beam is computed by

$$\delta\phi(t) = (\omega/c)\ell\beta\bar{u}(t) \quad (\text{D20})$$

with $\beta = \partial n / \partial T$. This equation is equivalent to Eq. (3.2) in the limit $\ell\Omega \ll c$, in which case the retardation term $n_i(z - z')/c$ in Eq. (3.2) can be omitted (i.e., we neglect the light travel time through the crystal). This approximation holds even for meter-scale optics so long as $\Omega/2\pi \lesssim 50$ MHz. Thus we arrive at the limiting form,

$$S_{e_x e_x}(\Omega) = \left| \frac{k\ell\epsilon'_{xx}}{2n_x} \langle e_x^{(0)} \rangle \right|^2 S_{\bar{u}\bar{u}}(\Omega), \quad (\text{D21})$$

valid in the adiabatic regime. Note that we cannot arrive at a similar limiting expression for $S_{e_y e_y}$ or $S_{e_x e_y}$ using the modal expansion method because the assumption that only the $n = 0$ mode contributes to \bar{u} no longer holds.

5. Adiabatic limit: Direct method

We now perform a second independent check of our formalism by modeling the transmission problem using

Levin's approach via the fluctuation-dissipation theorem [61,62].

Levin directly computes the spectral density of an *ad hoc* observable,

$$\int dV q(\mathbf{r}) \delta u(\mathbf{r}, t), \quad (\text{D22})$$

whose form is intuited to reflect the transduction of local temperature fluctuations to the relevant optical property. We take δe_x to be the observable of interest, in which case,

$$q(\mathbf{r}) = \frac{k\epsilon'_{xx} \langle e_x^{(0)} \rangle}{2\pi n_x r_0^2} \exp \left[-\frac{x^2 + y^2}{r_0^2} \right]. \quad (\text{D23})$$

This is read off from Eq. (3.2).

Next, Levin studies how a sinusoidal injection of entropy,

$$\frac{\delta s}{\delta V} = F_0 q(\mathbf{r}) \cos \Omega t, \quad (\text{D24})$$

is distributed in the medium via thermal dissipation. This can be done in the anisotropic case by solving the sinusoidally-driven heat equation,

$$(\partial_t - D_{ij} \partial_i \partial_j) \delta T = \frac{T}{c_V} \frac{\partial}{\partial t} \left(\frac{\delta s}{\delta V} \right), \quad (\text{D25})$$

with insulating boundary conditions at $z = 0, \ell$. The required solution is

$$\delta T = \frac{k\epsilon'_{xx} \langle e_x^{(0)} \rangle F_0 \Omega}{4in_x c_V} \int_{-\infty}^{+\infty} \frac{dk_x dk_y}{(2\pi)^2} \times \left[\frac{e^{i(\Omega t - k_x x - k_y y)} e^{-(k_x^2 + k_y^2)r_0^2/4}}{i\Omega + \mathfrak{D}(k_x, k_y)} - \text{c.c.} \right]. \quad (\text{D26})$$

It is in this step that our approach diverges from that of Levin's. We solve for the stochastic local temperature field by augmenting the thermal transport equation with a source that is consistent with the known equilibrium temperature

fluctuation (essentially a fluctuation-dissipation theorem for the temperature). We then propagate that local temperature field through its impact on the electromagnetic field. Levin directly applies the fluctuation-dissipation theorem to the *ad hoc* observable.

To do so, it is necessary to compute the dissipated energy. In the anisotropic case, it is

$$W_{\text{diss}} = \int dV \frac{\kappa_{ij}}{T} \langle \partial_i(\delta T) \partial_j(\delta T) \rangle. \quad (\text{D27})$$

Knowing the dissipated energy, the fluctuation-dissipation theorem can be applied to derive the spectral density of the observable,

$$S_{e_x e_x} = \frac{8k_B T W_{\text{diss}}}{\Omega^2 F_0^2} = \left| \frac{k\ell \epsilon'_{xx}}{2n_x} \langle e_x^{(0)} \rangle \right|^2 S_{\bar{u}\bar{u}}(\Omega), \quad (\text{D28})$$

where $S_{\bar{u}\bar{u}}$ is given by Eq. (D19). As expected, Levin's method and the first principles calculations agree in the adiabatic limit.

-
- [1] G. Harry, T. Bodiya, and R. De Salvo, *Optical Coatings and Thermal Noise in Precision Measurement* (Cambridge University Press, Cambridge, England, 2012).
- [2] W. H. Glenn, Noise in interferometric optical systems: An optical Nyquist theorem, *IEEE J. Quantum Electron.* **25**, 1218 (1989).
- [3] K. H. Wanser, Fundamental phase noise limit in optical fibres due to temperature fluctuations, *Electron. Lett.* **28**, 53 (1992).
- [4] V. B. Braginsky, M. L. Gorodetsky, and S. P. Vyatchanin, Thermo-refractive noise in gravitational wave antennae, *Phys. Lett. A* **271**, 303 (2000).
- [5] M. Evans, S. Ballmer, M. Fejer, P. Fritschel, G. Harry, and G. Ogin, Thermo-optic noise in coated mirrors for high-precision optical measurements, *Phys. Rev. D* **78**, 102003 (2008).
- [6] K. H. Wanser, A. D. Kersey, and A. Dandridge, Intrinsic thermal phase noise limit in optical fiber interferometers, *Opt. Photonics News* **4**, 37 (1993).
- [7] S. Foster, G. A. Cranch, and A. Tikhomirov, How sensitive is the fibre laser strain sensor?, in *19th International Conference on Optical Fibre Sensors* (International Society for Optics and Photonics, 2008), Vol. 7004, p. 70043J, 10.1117/12.785936.
- [8] S. Foster, A. Tikhomirov, and M. Milnes, Fundamental thermal noise in distributed feedback fiber lasers, *IEEE J. Quantum Electron.* **43**, 378 (2007).
- [9] S. Foster, G. A. Cranch, and A. Tikhomirov, Experimental evidence for the thermal origin of $1/f$ frequency noise in erbium-doped fiber lasers, *Phys. Rev. A* **79**, 053802 (2009).
- [10] M. L. Gorodetsky and I. S. Grudin, Fundamental thermal fluctuations in microspheres, *J. Opt. Soc. Am. B* **21**, 697 (2004).
- [11] G. Anetsberger, E. Gavartin, O. Arcizet, Q. P. Unterreithmeier, E. M. Weig, M. L. Gorodetsky, J. P. Kotthaus, and T. J. Kippenberg, Measuring nanomechanical motion with an imprecision below the standard quantum limit, *Phys. Rev. A* **82**, 061804(R) (2010).
- [12] N. L. Thomas, A. Dhakal, A. Raza, F. Peyskens, and R. Baets, Impact of fundamental thermodynamic fluctuations on light propagating in photonic waveguides made of amorphous materials, *Optica* **5**, 328 (2018).
- [13] G. Huang, E. Lucas, J. Liu, A. S. Raja, G. Lihachev, M. L. Gorodetsky, N. J. Engelsens, and T. J. Kippenberg, Thermorefractive noise in silicon-nitride microresonators, *Phys. Rev. A* **99**, 061801(R) (2019).
- [14] T. E. Drake, J. R. Stone, T. C. Briles, and S. B. Papp, Thermal decoherence and laser cooling of Kerr microresonator solitons, *Nat. Photonics* **14**, 480 (2020).
- [15] C. Panuski, D. Englund, and R. Hamerly, Fundamental Thermal Noise Limits for Optical Microcavities, *Phys. Rev. X* **10**, 041046 (2020).
- [16] V. B. Braginsky and S. P. Vyatchanin, Thermodynamical fluctuations in optical mirror coatings, *Phys. Lett. A* **312**, 244 (2003).
- [17] K. Numata, M. Ando, K. Yamamoto, S. Otsuka, and K. Tsubono, Wide-Band Direct Measurement of Thermal Fluctuations in an Interferometer, *Phys. Rev. Lett.* **91**, 260602 (2003).
- [18] K. Numata, A. Kemery, and J. Camp, Thermal-Noise Limit in the Frequency Stabilization of Lasers with Rigid Cavities, *Phys. Rev. Lett.* **93**, 250602 (2004).
- [19] M. Notcutt, L.-S. Ma, A. D. Ludlow, S. M. Foreman, J. Ye, and J. L. Hall, Contribution of thermal noise to frequency stability of rigid optical cavity via Hertz-linewidth lasers, *Phys. Rev. A* **73**, 031804(R) (2006).
- [20] D. G. Matei, T. Legero, S. Häfner, C. Grebing, R. Weyrich, W. Zhang, L. Sonderhouse, J. M. Robinson, J. Ye, F. Riehle, and U. Sterr, 1.5 μm Lasers with Sub-10 mHz Linewidth, *Phys. Rev. Lett.* **118**, 263202 (2017).
- [21] G. M. Harry, A. M. Gretarsson, P. R. Saulson, S. E. Kittelberger, S. D. Penn, W. J. Startin, S. Rowan, M. M. Fejer, D. R. M. Crooks, G. Cagnoli, J. Hough, and N. Nakagawa, Thermal noise in interferometric gravitational wave detectors due to dielectric optical coatings, *Classical Quantum Gravity* **19**, 897 (2002).
- [22] A. E. Villar, E. D. Black, R. DeSalvo, K. G. Libbrecht, C. Michel, N. Morgado, L. Pinard, I. M. Pinto, V. Pierro, V. Galdi, M. Principe, and I. Taurasi, Measurement of thermal noise in multilayer coatings with optimized layer thickness, *Phys. Rev. D* **81**, 122001 (2010).
- [23] T. Chalermongsak, F. Seifert, E. D. Hall, K. Arai, E. K. Gustafson, and R. X. Adhikari, Broadband measurement of coating thermal noise in rigid fabry-pérot cavities, *Metrologia* **52**, 17 (2014).

- [24] S. Gras, H. Yu, W. Yam, D. Martynov, and M. Evans, Audio-band coating thermal noise measurement for advanced ligo with a multimode optical resonator, *Phys. Rev. D* **95**, 022001 (2017).
- [25] M. Granata, A. Amato, G. Cagnoli, M. Coulon, J. Degallaix, D. Forest, L. Mereni, C. Michel, L. Pinard, B. Sassolas, and J. Teillon, Progress in the measurement and reduction of thermal noise in optical coatings for gravitational-wave detectors, *Appl. Opt.* **59**, A229 (2020).
- [26] V. B. Braginsky, M. L. Gorodetsky, and S. P. Vyatchanin, Thermodynamical fluctuations and photo-thermal shot noise in gravitational wave antennae, *Phys. Lett. A* **264**, 1 (1999).
- [27] E. Verhagen, S. Deleglise, S. Weis, A. Schliesser, and T. J. Kippenberg, Quantum-coherent coupling of a mechanical oscillator to an optical cavity mode, *Nature (London)* **482**, 63 (2012).
- [28] G. D. Cole, W. Zhang, M. J. Martin, J. Ye, and M. Aspelmeyer, Tenfold reduction of Brownian noise in high-reflectivity optical coatings, *Nat. Photonics* **7**, 644 (2013).
- [29] T. Chalermongsak, E. D. Hall, G. D. Cole, D. Follman, F. Seifert, K. Arai, E. K. Gustafson, J. R. Smith, M. Aspelmeyer, and R. X. Adhikari, Coherent cancellation of photothermal noise in GaAs/Al 0.92 Ga 0.08 As Bragg mirrors, *Metrologia* **53**, 860 (2016).
- [30] Y. T. Liu and K. S. Thorne, Thermoelastic noise and homogeneous thermal noise in finite sized gravitational-wave test masses, *Phys. Rev. D* **62**, 122002 (2000).
- [31] M. Cerdonio, L. Conti, A. Heidmann, and M. Pinard, Thermoelastic effects at low temperatures and quantum limits in displacement measurements, *Phys. Rev. D* **63**, 082003 (2001).
- [32] M. L. Gorodetsky, Thermal noises and noise compensation in high-reflection multilayer coating, *Phys. Lett. A* **372**, 6813 (2008).
- [33] A. Gurkovsky and S. P. Vyatchanin, The thermal noise in multilayer coating, *Phys. Lett. A* **374**, 3267 (2010).
- [34] T. Hong, H. Yang, E. K. Gustafson, R. X. Adhikari, and Y. Chen, Brownian thermal noise in multilayer coated mirrors, *Phys. Rev. D* **87**, 082001 (2013).
- [35] J. Alnis, A. Schliesser, C. Y. Wang, J. Hofer, T. J. Kippenberg, and T. W. Hänsch, Thermal-noise-limited crystalline whispering-gallery-mode resonator for laser stabilization, *Phys. Rev. A* **84**, 011804(R) (2011).
- [36] J. Yu, D. Kedar, S. Häfner, T. Legero, F. Riehle, S. Habers, D. Nicolodi, C. Y. Ma, J. M. Robinson, E. Oelker, J. Ye, and U. Sterr, Excess noise in highly reflective crystalline mirror coatings, [arXiv:2210.15671](https://arxiv.org/abs/2210.15671).
- [37] J. L. Hall, J. Ye, and L.-S. Ma, Measurement of mirror birefringence at the sub-ppm level: Proposed application to a test of QED, *Phys. Rev. A* **62**, 013815 (2000).
- [38] F. Bielsa, A. Dupays, M. Fouche, R. Battesti, C. Robilliard, and C. Rizzo, Birefringence of interferential mirrors at normal incidence, *Appl. Phys. B* **97**, 457 (2009).
- [39] M. Durand, J. Morville, and D. Romanini, Shot-noise-limited measurement of sub-parts-per-trillion birefringence phase shift in a high-finesse cavity, *Phys. Rev. A* **82**, 031803 (R) (2010).
- [40] G. Bailly, R. Thon, and C. Robilliard, Highly sensitive frequency metrology for optical anisotropy measurements, *Rev. Sci. Instrum.* **81**, 033105 (2010).
- [41] A. J. Fleisher, D. A. Long, Q. Liu, and J. T. Hodges, Precision interferometric measurements of mirror birefringence in high-finesse optical resonators, *Phys. Rev. A* **93**, 013833 (2016).
- [42] A. Ejlli, F. Della Valle, U. Gastaldi, G. Messineo, R. Pengo, G. Ruoso, and G. Zavattini, The pvlas experiment: A 25 year effort to measure vacuum magnetic birefringence, *Phys. Rep.* **871**, 1 (2020).
- [43] C. Robilliard, R. Battesti, M. Fouche, J. Mauchain, A.-M. Sautivet, F. Amiranoff, and C. Rizzo, No “Light Shining Through a Wall”: Results from a Photoregeneration Experiment, *Phys. Rev. Lett.* **99**, 190403 (2007).
- [44] K. Ehret, M. Frede, S. Ghazaryan, M. Hildebrandt, E.-A. Knabbe, D. Kracht, A. Lindner, J. List, T. Meier, N. Meyer *et al.*, New alps results on hidden-sector lightweights, *Phys. Lett. B* **689**, 149 (2010).
- [45] I. Obata, T. Fujita, and Y. Michimura, Optical Ring Cavity Search for Axion Dark Matter, *Phys. Rev. Lett.* **121**, 161301 (2018).
- [46] H. Liu, B. D. Elwood, M. Evans, and J. Thaler, Searching for axion dark matter with birefringent cavities, *Phys. Rev. D* **100**, 023548 (2019).
- [47] N. M. Kondratiev, A. Gurkovsky, and M. L. Gorodetsky, Thermal noise and coating optimization in multilayer dielectric mirrors, *Phys. Rev. D* **84**, 022001 (2011).
- [48] W. Yam, S. Gras, and M. Evans, Multimaterial coatings with reduced thermal noise, *Phys. Rev. D* **91**, 042002 (2015).
- [49] J. Steinlechner, I. W. Martin, J. Hough, C. Krüger, S. Rowan, and R. Schnabel, Thermal noise reduction and absorption optimization via multimaterial coatings, *Phys. Rev. D* **91**, 042001 (2015).
- [50] M. Principe, Reflective coating optimization for interferometric detectors of gravitational waves, *Opt. Express* **23**, 10938 (2015).
- [51] S. C. Tait, J. Steinlechner, M. M. Kinley-Hanlon, P. G. Murray, J. Hough, G. McGhee, F. Pein, S. Rowan, R. Schnabel, C. Smith *et al.*, Demonstration of the Multimaterial Coating Concept to Reduce Thermal Noise in Gravitational-Wave Detectors, *Phys. Rev. Lett.* **125**, 011102 (2020).
- [52] V. Pierro, V. Fiumara, F. Chiadini, V. Granata, O. Durante, J. Neilson, C. Di Giorgio, R. Fittipaldi, G. Carapella, F. Bobba *et al.*, Ternary quarter wavelength coatings for gravitational wave detector mirrors: Design optimization via exhaustive search, *Phys. Rev. Res.* **3**, 023172 (2021).
- [53] V. Pierro, V. Fiumara, and F. Chiadini, Optimal design of coatings for mirrors of gravitational wave detectors: Analytic turbo solution via herpin equivalent layers, *Appl. Sci.* **11**, 11669 (2021).
- [54] V. Granata, V. Pierro, and L. Troiano, Meta-heuristics optimization of mirrors for gravitational wave detectors: Cryogenic case, *Appl. Sci.* **12**, 7680 (2022).
- [55] W. DeRocco and A. Hook, Axion interferometry, *Phys. Rev. D* **98**, 035021 (2018).
- [56] A. C. Melissinos, Proposal for a Search for Cosmic Axions using an Optical Cavity, *Phys. Rev. Lett.* **102**, 202001 (2009).

- [57] F. Della Valle, A. Ejlli, U. Gastaldi, G. Messineo, E. Milotti, R. Pengo, G. Ruoso, and G. Zavattini, The PVLAS experiment: Measuring vacuum magnetic birefringence and dichroism with a birefringent Fabry–Perot cavity, *Eur. Phys. J. C* **76**, 24 (2016).
- [58] R. Cameron, G. Cantatore, A. C. Melissinos, G. Ruoso, Y. Semertzidis, H. J. Halama, D. M. Lazarus, A. G. Prodell, F. Nezzrick, C. Rizzo, and E. Zavattini, Search for nearly massless, weakly coupled particles by optical techniques, *Phys. Rev. D* **47**, 3707 (1993).
- [59] L. D. Landau and E. M. Lifshitz, *Statistical Physics*, Course of Theoretical Physics Vol. 5 (Pergamon Press, New York, 1959).
- [60] K. M. van Vliet, Markov approach to density fluctuations due to transport and scattering. I. Mathematical formalism, *J. Math. Phys. (N.Y.)* **12**, 1981 (1971).
- [61] Y. Levin, Internal thermal noise in the LIGO test masses: A direct approach, *Phys. Rev. D* **57**, 659 (1998).
- [62] Y. Levin, Fluctuation–dissipation theorem for thermo-refractive noise, *Phys. Lett. A* **372**, 1941 (2008).
- [63] P. Morse and H. Feshbach, *Methods of Theoretical Physics* (McGraw-Hill, New York, 1953), Vol. II.
- [64] P. Morse and H. Feshbach, *Methods of Theoretical Physics* (McGraw-Hill, New York, 1953), Vol. I.
- [65] O. Korotkova and E. Wolf, Generalized Stokes parameters of random electromagnetic beams, *Opt. Lett.* **30**, 198 (2005).
- [66] P. Flubacher, A. J. Leadbetter, and J. A. Morrison, The heat capacity of pure silicon and germanium and properties of their vibrational frequency spectra, *Philos. Mag.* **4**, 273 (1959).
- [67] C. J. Glassbrenner and G. A. Slack, Thermal conductivity of silicon and germanium from 3°k to the melting point, *Phys. Rev.* **134**, A1058 (1964).
- [68] B. J. Frey, D. B. Leviton, and T. J. Madison, Temperature-dependent refractive index of silicon and germanium, in *Optomechanical Technologies for Astronomy* edited by E. Atad-Ettinger, J. Antebi, and D. Lemke, International Society for Optics and Photonics (SPIE, 2006), Vol. 6273, pp. 790–799.
- [69] J. Komma, C. Schwarz, G. Hofmann, D. Heinert, and R. Nawrodt, Thermo-optic coefficient of silicon at 1550 nm and cryogenic temperatures, *Appl. Phys. Lett.* **101**, 041905 (2012).
- [70] D. N. Nikogosyan, *Nonlinear Optical Crystals: A Complete Survey*, 1st ed. (Springer, New York, 2005).
- [71] D. E. Zelmon, D. L. Small, and D. Jundt, Infrared corrected sellmeier coefficients for congruently grown lithium niobate and 5 mol.% magnesium oxide–doped lithium niobate, *J. Opt. Soc. Am. B* **14**, 3319 (1997).
- [72] L. Moretti, M. Iodice, F. G. Della Corte, and I. Rendina, Temperature dependence of the thermo-optic coefficient of lithium niobate, from 300 to 515 k in the visible and infrared regions, *J. Appl. Phys.* **98**, 036101 (2005).
- [73] S. Adachi, *Properties of Aluminium Gallium Arsenide* (Institute of Electrical Engineers, London, 1993).
- [74] M. A. Fromowitz, Refractive index of $ga_{1-x}al_xas$, *Solid State Commun.* **15**, 59 (1974).
- [75] J. P. Kim and A. M. Sarangan, Temperature-dependent sellmeier equation for the refractive index of $al_xga_{1-x}as$, *Opt. Lett.* **32**, 536 (2007).
- [76] B. Benthem and Y. Levin, Thermorefractive and thermochemical noise in the beamsplitter of the geo600 gravitational-wave interferometer, *Phys. Rev. D* **80**, 062004 (2009).
- [77] G. Rempe, R. Lalezari, R. J. Thompson, and H. J. Kimble, Measurement of ultralow losses in an optical interferometer, *Opt. Lett.* **17**, 363 (1992).
- [78] M. Born and E. Wolf, *Principles of Optics*, 7th ed. (Cambridge University Press, Cambridge, England, 1999).
- [79] L. D. Landau, E. M. Lifshitz, and L. P. Pitaevskii, *Electrodynamics of Continuous Media*, Course of Theoretical Physics Vol. 8 (Pergamon Press, New York, 1984).
- [80] G. R. Fowles, *Introduction to Modern Optics*, 2nd ed. (Dover Publications, New York, 1975).
- [81] D. Z. Anderson, Alignment of resonant optical cavities, *Appl. Opt.* **23**, 2944 (1984).
- [82] For silica, we take $\partial n/\partial T = 11 \text{ ppmK}^{-1}$, $\kappa = 1.4 \text{ Wm}^{-1} \text{K}^{-1}$, and $c_V = 1.6 \times 10^6 \text{ Jm}^{-3} \text{K}^{-1}$.
- [83] L. Mandel, E. C. Sudarshan, and E. Wolf, Theory of photoelectric detection of light fluctuations, *Proc. Phys. Soc. London* **84**, 435 (1964).
- [84] In fact, complete information is contained in any linearly independent combination of polarization states, which can be extracted in principle if the photocurrents are combined with unequal weights.
- [85] W. Phillips, Two-level states in glasses, *Rep. Prog. Phys.* **50**, 1657 (1987).
- [86] R. O. Pohl, X. Liu, and E. Thompson, Low-temperature thermal conductivity and acoustic attenuation in amorphous solids, *Rev. Mod. Phys.* **74**, 991 (2002).
- [87] R. Bassiri, K. Evans, K. B. Borisenko, M. M. Fejer, J. Hough, I. MacLaren, I. W. Martin, R. K. Route, and S. Rowan, Correlations between the mechanical loss and atomic structure of amorphous tio_2 -doped ta_2o_5 coatings, *Acta Mater.* **61**, 1070 (2013).
- [88] J. P. Trinastic, R. Hamdan, C. Billman, and H.-P. Cheng, Molecular dynamics modeling of mechanical loss in amorphous tantalum and titania-doped tantalum, *Phys. Rev. B* **93**, 014105 (2016).
- [89] M. Stoehr, G. Gerlach, T. Härtling, and S. Schoenfelder, Analysis of photoelastic properties of monocrystalline silicon, *J. Sens. Sens. Syst.* **9**, 209 (2020).
- [90] V. B. Braginsky and S. P. Vyatchanin, Corner reflectors and quantum nondemolition measurements in gravitational wave antennae, *Phys. Lett. A* **324**, 345 (2004).
- [91] N. N. Lebedev, *Special Functions & Their Applications* (Dover, New York, 1972).
- [92] We use asymptotic notation in the following sense: $f(a) = O(g(a))$ means that $\lim_{x \rightarrow a} |f/g| < \infty$; $f(a) = o(g(a))$ means that $\lim_{x \rightarrow a} |f/g| = 0$; and $f(a) \sim g(a)$ means that $\lim_{x \rightarrow a} |f/g| = 1$.